THE DESIGN AND TESTING OF AN AERODYNAMIC MODEL OF A HIGH SPEED WIND TUNNEL

Thesis by

Richard S. Shevell

In Partial Fulfillment of the Requirements for the Degree of Aeronautical Engineer

California Institute of Technology
Pasadena, California
1942

Acknowledgements

I wish to express my deepest gratitude to Dr.Clark B.Millikan who has been a source of inspiration and encouragement throughout the course of this research. I also wish to thank Dr.H.W.Liepmann,Dr.H.S.Tsien,and Mr. Carl Thiele for their valuable advice on many phases of the work.Grateful acknowledgement is also made to Mr.J.C.Schwartzenbach whose assistance during the experimental investigation was invaluable.

Table of Contents

Summary

In conjunction with the design of the high speed Cooperative Wind Tunnel at the California Institute of Technology an aerodynamic model was built and tested. Methods of design of the contraction, working section, and diffuser are explained.

The model test showed that the working section of a wind tunnel operating at a Mach Number greater than 0.7 must have adjustable walls to maintain a constant velocity through the working section. The unsatisfactory design of the diffuser is demonstrated by both static pressure measurements and visual observations.

A description is given of visual observations of supersonic phenomena occurring in the working section and diffuser of the model.

Introduction

With the advent of higher airplane flight velocities, the need for aerodynamic laboratories capable of matching full scale conditions has increased. At airplane speeds greater than 300 miles per hour local velocities over some parts of the airplane, such as the upper surface of the wing, may approach or even exceed the velocity of sound. When the Mach Number, the ratio of the local velocity to the speed of sound, approaches unity, phenomena completely unexplained by perfect fluid theory considerations occur. If such "compressibility" effects are possible it is no longer sufficient to extrapolate wind tunnel test results to full scale Reynolds Number. The parameter upon which the occurrence of such compressibility effects depends, that is, the Mach Number, has become as important, or more so, than the scale effect, and it is necessary to run such tests at full scale Mach Number if the results are to be useful in the high speed range.

The Cooperative Wind Tunnel now being designed at the California Institute of Technology to meet this research problem is expected to operate at speeds approaching 750 m.p.h. The aerodynamic design of such a wind tunnel involves problems not encountered with velocities under the range in which the effects of the compressibility of air become important. The present paper is concerned with the methods of designing the contraction, working section, and diffuser of the Cooperative Wind Tunnel, and with an experimental investigation on a small scale model of these components of the tunnel operated at full scale velocities.

Before beginning such a wind tunnel design it is necessary to select a criterion upon which desirable characteristics are known, or assumed, to depend. In general we know from both theoretical and empirical considerations that certain pressure and velocity distributions along the length of the tunnel will lead to satisfactory flow characteristics. The first problem is then to choose the desired velocity and pressure distributions. Given these it is then possible by use of the equations of flow for a compressible fluid to solve for the cross-section area distribution along the tunnel which will give the desired velocity and pressure gradients. The method used will be outlined below. A suitable list of references is included on page 47 so that only the results of the theory of compressible fluid flow will be given here.

Theory and Method of Design

The effect of the compressible character of air on design problems can best be shown by consideration of the fundamental relations between velocity, pressure, density, and the cross-section area of a stream tube.

The following notation shall be used:

S = cross-section area

p = pressure

ρ = density

V = velocity

k = ratio of the specific heat at constant pressure to the specific heat at constant volume.

Basic Equations

Bernoulli's equation for a compressible fluid is

1) $$\frac{V^2}{2} + \frac{K}{K-1}\frac{p}{\rho} = \frac{V_o^2}{2} + \frac{K}{K-1}\frac{p_o}{\rho_o}$$

Differentiating this we find

$$V + \frac{K}{K-1}\left(\frac{1}{\rho}\frac{dp}{d\rho} - \frac{p}{\rho^2}\right)\frac{d\rho}{dV} = 0$$

2) or

$$V + \frac{C^2}{\rho}\frac{d\rho}{dV} = 0$$

From the continuity equation, ρVS = constant,

3) $$\frac{1}{S}\frac{dS}{dV} + \frac{1}{\rho}\frac{d\rho}{dV} + \frac{1}{V} = 0$$

Substituting 2) in 3) gives

4) $$\frac{dS}{S} = -\left(1 - \frac{V^2}{C^2}\right)\frac{dV}{V}$$

$$= -(1 - M^2)\frac{dV}{V}$$

where

C = velocity of sound

$M = \frac{V}{C}$ = Mach Number

Thus the ratio between the percentage change of velocity and the corresponding percentage change of area is dependent upon the Mach Number, M. It is seen that as M approaches 1, a small change in area will result in a large change in velocity. From the Bernoulli relation it is seen that this will in turn cause a large change in pressure. If we then desire certain velocity and pressure gradients to be constant regardless of the Mach Number we must vary the area much more slowly at higher velocities. This fact is the basis of the design of a diffuser for a high speed wind tunnel. For the same rate of velocity change as in an incompressible diffuser the rate of area expansion must be very much smaller at high Mach Numbers, and therefore just aft of the working section a small divergence angle is used. As the velocity decreases in the diffuser, the Mach Number similarly decreases and the divergence angle may be increased even though the

pressure gradient or similar criteria is held constant along the length of the diffuser.

If we add to the Bernoulli equation and the continuity equation, the adiabatic relation

5) $$\frac{p}{p_0} = \left(\frac{\rho}{\rho_0}\right)^K$$

we have set up the fundamental formulae required for working with compressible flow at subsonic speeds in a channel assumed for calculation purposes to be one dimensional. Except for the region of large curvature of the walls in the contraction, the assumption of one dimensional flow in a wind tunnel is satisfactory and the Bernoulli equation (1) may be used.

It is convenient to use the point along the channel at which sonic velocity would be reached as a reference. From equation 4) we see that sonic velocity can exist only at the cross-section of least area. Actually in this design we do not expect to reach sonic velocity, but we can consider an imaginary cross-section of smaller area downstream of the entrance of the working section, so that sonic velocity is actually reached at this fictitious "minimum" section. The method is to use this fictitious minimum section as a reference and then effectively consider the channel only as close to this minimum section as we wish to go. Then from equation 1) letting $(\ )_m$ indicate the minimum section where $v = C_m$

6) $$(K-1)\,V^2 + 2\,C^2 = (K+1)\,C_m^2$$

Also

$$\left(\frac{p}{p_m}\right)^{\frac{K-1}{K}} = \left(\frac{\rho}{\rho_m}\right)^{K-1} = \left(\frac{C}{C_m}\right)^2$$

Finally from continuity

$$\left(\frac{S_m}{S}\right)^{K-1} = \left(\frac{\rho V}{\rho_m V_m}\right)^{K-1}$$

$$= \frac{C^2}{C_m^2}\left(\frac{V}{C_m}\right)^{K-1}$$

Substituting from (6)

7) $$\left(\frac{S_m}{S}\right)^{K-1} = \frac{K+1}{2}\left(\frac{V}{C_m}\right)^{K-1} - \frac{K-1}{2}\left(\frac{V}{C_m}\right)^{K+1}$$

This relation (7) determines the ratio between the area at any section and the area at the minimum section in terms of the velocity ratio at the two sections, and is the equation used to convert the desired velocity and pressure conditions into area distribution.

Contraction Design

It was decided to design the contraction on the assumption of a Mach Number of 0.9 at the entrance of the working section. The subscript "w" shall indicate conditions at the entrance of the working section. We are then given

$$M_w = \frac{V_w}{C_w} = 0.9$$

Dividing equation (6) by C gives a relation between C_w/C_m and the Mach Number at the working section. It is now possible to find the ratio of V_x (at any point, x, along the tunnel axis) to C_m, the velocity at the fictitious minimum section. This is given since

8) $$\frac{V_x}{C_m} = \frac{V_x}{V_w} \times \frac{V_w}{C_w} \times \frac{C_w}{C_m}$$

Of the terms on the right-hand side, the first is assumed when we choose the velocity distribution, the second is simply the Mach Number at the working section, and the third is a function of this Mach Number as given by equation (6).

Before assuming the curve of $\frac{V_x}{V_w}$ it is necessary to determine the endpoints of the curve. At the working section the ratio equals 1 by definition. We cannot proceed further until we find $\frac{V_x}{V_w}$ at the beginning of the contraction.

First, the area of the cross-section at the beginning and end of the contraction must be determined. This is, of course, a function of the contraction ratio and the area of the working section. For this design a rectangular working section 8.5 ft. by 12 ft. with filleted corners had been selected. Its cross-section area was 95.7 ft.^{2}. The contraction ratio was 8.21 so that the area of the section at the entrance of the contraction was fixed at 779 ft.^{2}. In addition the axial length of the contraction was specified as being 26 ft.

It was convenient to work with effective diameters rather than areas. Effective diameter is defined as the diameter of the

circular cross-section which has the same area as the section of the tunnel in question. A curve of $\frac{D_x}{D_m}$ as a function of $\frac{V_x}{C_m}$ was computed from equation(7). This will be useful only when D_m is known. Solving for $\frac{V_w}{C_m}$ we find

$$\frac{V_w}{C_m} = \frac{V_w}{C_w} \times \frac{C_w}{C_m}$$

From the curve of equation (7) we can find $\frac{D_w}{D_m}$ and then solve for D_m since D_w is known.

Knowing the diameter at the section ahead of the contraction to be equal to 31.5 ft. we calculate $\frac{D_{31.5}}{D_m}$ and find $\frac{V_{31.5}}{C_m}$. We can then calculate $\frac{V_{31.5}}{V_w}$.

The endpoints of the velocity distribution curve have now been determined. It remains to draw a smooth velocity curve between these endpoints. The purpose of a contraction is to accelerate the air and to deliver a flow with uniform velocity distribution across the section at the entrance of the working section. It would seem that a smooth and continuous acceleration would be desirable to achieve this. Thus a velocity curve was selected which gives a constant acceleration over most of the contraction with a gradual rate of change of acceleration at the beginning and end of the contraction. This curve is shown in Fig. 1 .

We now have $\frac{V_x}{V_w}$ at every point in the contraction. By equation 8) we find $\frac{V_x}{C_m}$. From the curve of equation 7, we pick off $\frac{D_x}{D_m}$. Multiplying by the effective diameter at the minimum section gives the desired diameter at every station. The curve of effective radius is also shown on Fig. 1 .

Diffuser Design

The selection of a diffuser is a compromise between the diffuser with the least energy loss during the transformation of kinetic into pressure energy and the diffuser with the least length. The optimum diffuser has a divergence angle of about 6 degrees. Diffusers with divergence angles of greater than 9 degrees are likely to produce a separation of the flow from the walls with an attendant loss of energy. At the same time the diffuser with the smaller angle must be considerably longer in order to achieve the same energy transformation from kinetic to pressure energy. The first cost of increasing the overall length of a wind tunnel of a longer diffuser may outweigh the saving in operating costs due to an increase of the energy ratio. In addition the longer diffuser has greater frictional losses.

For the Cooperative Wind Tunnel a compromise diffuser was selected. From early estimate of the tunnel dimensions the overall length of the diffuser was specified. In order to reduce the high

losses at the first corner after the diffuser, as low a velocity as possible was desired at the end of the diffuser so that a diameter of 18.5 ft. was chosen. Thus the length and the end dimensions were given and the problem was to design, if possible, a suitable diffuser to fit these conditions.

After much consideration of the problem it was decided to choose a diffuser known to be satisfactory for an effectively incompressible fluid, such as air at relatively low speeds, and to match some parameter, which would be assumed to determine roughly at least the separation characteristics of the diffuser, in a diffuser design for a compressible fluid, such as air at high velocities.

The parameter selected was $\frac{1}{V/V_w}\frac{d(V/V_w)}{dx}$. By differentiating Bernouilli's equation for an incompressible fluid it is seen that this parameter is proportional to $\frac{\frac{dp}{dx}}{\rho/2\, V^2}$. Although there is no generally accepted separation criteria which is readily usable in diffuser design, it was felt that $\frac{\frac{dp}{dx}}{\rho/2\, V^2}$ would be sufficiently representative of the pressure and velocity gradients in a diffuser to serve as an approximate guide. It should further be noted that the parameter, $\frac{1}{V/V_w}\frac{d(V/V_w)}{dx}$, is proportional to the ratio of the pressure gradient to the dynamic pressure only in an incompressible fluid. Differentiating Bernouilli's equation for a compressible fluid and solving for $\frac{dp}{dx}$ shows that with the same value of the selected parameter, the pressure gradient is greater

in a compressible fluid than in an incompressible fluid due to a term dependent upon $\frac{d\rho}{dx}$. Thus using this method of design will give a diffuser for a compressible fluid that is less conservative than the incompressible fluid diffuser upon which it is based.

The actual procedure used was to layout a six degree diffuser. From the area at each section and the continuity equation for an incompressible fluid a curve of $\frac{V_x}{V_w}$ can be drawn. Then the method is identical with that described for the contraction design. The parameter used in the contraction design was actually the same as in the diffuser with the exception of the fact that the values of the parameter used were assumed in the contraction design while they were chosen from a known incompressible case in the design of the critical diffuser.

During the course of the investigation of the diffuser area distribution several other parameters were considered. In addition the diffuser design was carried through in part for various Mach Numbers in the working section using the method outlined above. Unfortunately time did not permit the preparation of these results in a readily presentable form. It is interesting to note however that seventy feet downstream from the entrance of the diffuser the diameter of the diffuser varied from 18.4 ft. for the straight six degree incompressible diffuser to 14.9 ft. for the compressible fluid diffuser based on a six degree incompressible fluid diffuser and a Mach Number of 0.95 in the working section. It is quite clear that to achieve the

same velocity and pressure conditions for a high speed diffuser as in a diffuser satisfactory at low speeds, the length of the diffuser must be considerably increased.

It has been mentioned that the length and the end diameters of the diffuser were essentially fixed. Therefore in the light of the above discussion selection of a diffuser was difficult. It was decided to use the design of the diffuser based on a Mach Number of .85 in the working section for the first twenty-five feet of the length, and then to fair the diffuser smoothly into such a divergence angle as was necessary to meet the 18.5 ft. diameter near the first corner some 71 ft. downstream from the end of the working section. The resultant divergence angle was 8.2 degrees. In view of the fact that the design velocity in the region where the 8.2 degree diffuser started was of the order of 500 miles per hour, the Mach Number being about 0.7, this is quite large and corresponds to an incompressible fluid divergence angle of well over 9 degrees. The effective radius distribution is shown in Fig. 2 .

Working Section Design

The vertical walls of the working section were designed to be slightly divergent to correct for the thickening boundary layer in the section. The amount of divergence was calculated for a velocity of 300 m.p.h. using the displacement thickness of the expanding boundary layer as a measure of the effective area decrease

in the working section. The walls were displaced .625 inches and corrected for an effective area decrease of 0.92%.

The Aerodynamic Model

Because of the non-conservative design of the diffuser, the large accelerations in the contraction, and the high Mach Numbers at which the tunnel is expected to operate, it was considered advisable to construct an aerodynamic model of the contraction, working section, and the diffuser. The model was designed to reach the same velocities as the full scale tunnel. The power for the model was to be furnished by an air compressor system used at the GALCIT for high speed research. The scale of the model was determined by the capacity of the air compressors and was calculated to be 1 : 46.5.

The geometry of the working section has already been described as being rectangular. As the simplest procedure, and one allowing the use of only single curved surfaces in the full scale tunnel, geometrical similarity of the cross-section was maintained in both the contraction and the diffuser. The working section cross-section was in effect expanded so that the area distribution along the tunnel followed the calculated distributions. The contraction section was allowed to run into the 31.5 ft. cylindrical section upstream of the contraction. The flat walls of the diffuser similarly expanded until they disappeared in the 18.5 ft. cylinder

at the end of the diffuser. The only disadvantage of this system is that the vertical walls disappear first so that in the last part of the diffuser all the area expansion is taken up only by the top and bottom of the tunnel. This results in a rather large slope of these portions of the tunnel wall. The layout of the tunnel is shown in Fig.3.

Description of Equipment

The model of the tunnel was essentially a duct in a block of plaster-of-paris. From the layout of the contraction, working section, and diffuser, a male pattern of the tunnel was made. This pattern was constructed in two parts, with the parting line along the center of the vertical walls. (The upper half of the pattern is shown in Fig. 17 .) Castings of the upper and lower halves were made of plaster-of-paris. The two halves were placed together so that the final result was a block of plaster approximately three feet long with a cross-section area of about one square foot, and with the duct running through it. Cast in the upstream end was an 18-inch length of 8 in. diameter pipe which served as an entrance section.

Inserted in the lower half of the casting, flush with the floor of the working section of the tunnel, was a brass bearing into which could be inserted plugs carrying various types of experimental equipment. The two plugs designed and used included one with a total head tube for boundary layer measurements, and one with a small pitot-static tube for velocity measurements. In one vertical wall, along the parting line of the casting, another brass bearing was installed at the same section as the bearing in the floor in order that surveys could be made both horizontally as well as vertically across the tunnel working section. A similar provision

for surveys across the tunnel was made at a section several inches upstream of the entrance to the contraction. Here a total head tube for determining the velocity profile was used.

Static tubes with 1/32 inch internal diameter holes were set flush with the surface of one vertical wall and were spaced approximately every two inches from a point in the eight inch diameter section at the entrance to the contraction to a station .5 inch from the end of the diffuser. A total of 18 such tubes were used. The tubes consisted of 1/8 in. outside diameter tubing cast directly in the plaster.

The upper wall of the working section was a piece of plate glass cast with the model so that the pitot tubes in the section could be observed. A channel was cast from the top of the plaster block to the glass window. Similar channels were cast opposite the stations at which the brass inserts for the pitot tubes were installed to allow accessibility to the instruments.

The total head tube installation in the working section was designed for boundary layer measurements. The tube itself was of hypodermic tubing with a flattened entrance. Its position relative to the wall was adjusted by means of a micrometer head which fitted into the frame supporting the stem of the total head tube.

The pitot static tube was of unusually small dimensions. The overall diameter was .05 inch. The tube was not a standard design. The four static holes were placed about .25 inch back of the leading

edge and were spaced 45 degrees apart around the tube. The stem consisted of two concentric tubes, the outer one being the static tube and the inner one the total head. A special fitting was designed to allow convenient attachments for the rubber tubing connecting the pitot-static to the manometer. The pitot-static tube is shown in Fig. 4 .

A total head tube on a traversing arm was arranged at the exit of the diffuser. Traverses across the exit could be taken in both horizontal and vertical directions.

The finish of the inside surface of the model varied considerably in different portions of the tunnel. The difficulties with the surface arose chiefly from the parting line where the two halves of the casting joined, and from small imperfections in the castings themselves. In all cases wax was used as a filler. The wax was carefully rubbed flush with the surface, shellaced, and then lightly sandpapered. The contraction and the working section were in good condition. Some parts of the diffuser, however, had small surface waves along the parting line. Most of these disturbances were confined to the exit end of the diffuser where they were least likely to prove troublesome.

A multiple mercury manometer was used to obtain the static pressure readings where the pressure was below atmospheric pressure. Other static pressure readings as well as those of the

traversing pitot tubes and the pitot-static tube were read on U-tube manometers.

As mentioned above the air supply for the model was furnished by the high pressure tank and air compressor system. The 8 inch diameter pipe was joined to an outlet on this tank through a gate valve. Downstream of the gate valve were three 8 inch diameter screens to smooth out the flow at the entrance of the contraction. Pressure in the tank is maintained by the rotary air compressor. Speed control is obtained by a valve at the intake of the constant displacement compressor.

Experimental Results and Discussion

The tests made on the model were divided into the following groups:

1) Velocity distribution along the axis of the tunnel at various Mach Numbers.
2) Velocity surveys across the entrance of the contraction.
3) Velocity surveys across the working section.
4) Boundary layer surveys in the working section.
5) Velocity surveys across the exit of the diffuser.
6) Visual observations of flow in the diffuser.

The first group, the velocity distribution along the axis of the tunnel casts considerable light upon the results of some of the other tests. It will be considered separately, however, and referred to whenever necessary.

1) Velocity distribution along the axis of the tunnel at various Mach Numbers.

The tunnel was operated at various constant velocities and the static pressure along the tunnel was recorded. The data are presented in several ways. Fig. 6 shows the variation of p/p_o along the tunnel. p is the absolute static pressure at the wall and p_o is the stagnation pressure. The latter was found by measuring the static pressure upstream of the entrance of the contraction and adding to it the dynamic pressure at that section.

At low Mach Numbers the curves are entirely normal with an essentially constant pressure throughout the length of the working section. It will be noted that the reading near the center of the working section is consistently slightly high. Due to the sensitivity of static pressure readings to the disturbances caused by surface roughness upstream from the tube orifice, it is felt that such small variations cannot be interpreted as being characteristic of the model design. It is known that since the static tubes were near the parting line of the model it is likely that such disturbances were present.

As the velocity increases the uniform pressure in the working section is no longer maintained. At p/p_o less than .65 the pressure decreases gradually along the length of the working section. As the velocity is increased the rate of pressure decrease becomes greater until the change in pressure along the working section is a considerable percentage of the total pressure drop from the stagnation pressure. At the highest velocity the minimum pressure point occurs beyond the working section in the beginning of the diffuser.

Now p/p_o is a direct function of the Mach Number. The relation is

$$\frac{p}{p_o} = \left[1 + \frac{K-1}{2} M^2\right]^{-3.5}$$

This equation is plotted in Fig. 5 . The results were reduced from p/p_o to Mach Number by use of this curve. The variation

of Mach Number was then plotted in Fig. 7 . The curves are very similar to those of the previous figure except that they are inverted. The results are most useful in this form. It is seen that the velocity distribution is quite uniform along the length of the working section up to M = 0.7. At higher Mach Numbers an increase in velocity occurs. Above M = 0.85 this increase is very marked. At M = 0.9 the Mach Number variation through the working section is about 10%.

These results are consistent throughout and check previously reported results very well. J. Ackeret [1] has carried out similar tests at high velocities and has presented his data in the form of Fig. 6 . Ackeret's curves are very similar to this figure in appearance and in the values of p/p_o at which large pressure variations occur in the working section. It has also been reported that full scale high speed wind tunnels recently constructed in this country have experienced the same effect of large variations at values of M greater than 0.8.

The meaning of this effect is clear if we refer to equation (4). As M approaches 1 the change in speed resulting from a small change in area becomes very large. Below M = 0.6 this effect is relatively small, but at a Mach Number of 0.9 a 1% decrease in cross section area will increase the Mach Number by 10%. The decrease in cross-section area caused by the growth of the boundary layer is of the order of 1%. Although the working section walls were slightly diverged

to take into account this boundary layer thickening, the calculations were based on the full scale dimensions at a velocity of 300 m.p.h. Thus the calculated divergence is for a Reynolds Number about 12 times that of the model, and the divergence is accordingly too small. This effect is not appreciable at low velocities where the percentage change in velocity is of the order of the percentage change in area. At high velocities, however, it is very considerable.

When a Mach Number of 1 is reached at the minimum cross-section at the downstream end of the working section, the character of the flow upstream of this point is changed. At lower velocities the manometer tubes connected to the contraction and working section were always mildly fluctuating. Most probably this was due to the transmission of disturbances in the diffuser upstream to the working section and contraction where variations in velocity resulted. After M reaches a value of 1, disturbances downstream of this point cannot travel upstream since the air is flowing faster than the disturbances can travel. The velocity cannot exceed that of sound at the minimum section and therefore conditions behind the minimum section are stabilized. This is reflected by the manometer mercury columns. Those tubes connected upstream of the point of sonic velocity become completely quiet in marked contrast to their previous condition. Tubes downstream of the position where sonic velocity exists fluctuate considerably, especially the tube just after the point of maximum velocity.

If sonic velocity is reached at the minimum section, the flow becomes supersonic in the diffuser. A shockwave then occurs, and apparently the shock moves back and forth along the tunnel in the vicinity of one of the static orifices. This disturbance causes very large fluctuations in the reading of the static pressure tube affected, and locates in an approximate manner the position of the shock. The shock was placed five to ten feet, full scale, downstream of the entrance of the diffuser.

In Fig. 8 the variation of $\frac{p - p_w}{q_w}$ is plotted.

This parameter was chosen because in an incompressible, frictionless fluid it is dependent only upon the ratio of the cross-section area at any point to the working section area. Thus from Bernoulli's equation for an incompressible fluid,

$$p - p_w = \frac{\rho}{2}\left(V_w^2 - V^2\right)$$

$$= \frac{\rho}{2} V_w^2 \left(1 - \left(\frac{S_w}{S}\right)^2\right)$$

letting $\frac{\rho}{2} V_w^2 = q_w$

$$\frac{p - p_w}{q_w} = 1 - \left(\frac{S_w}{S}\right)^2$$

All curves of $\frac{p - p_w}{q_w}$ vs. position along the tunnel should then coincide for a perfect fluid regardless of velocity. The calculated incompressible fluid curve is plotted and it is seen that the deviations of the experimental curves from the calculated

curve are large.

In the contraction the curves approach the calculated curve with decreasing velocity. The lowest velocity drops below the calculated curve. It is difficult to see how this would be possible since it seems to correspond to the lowest velocity condition having less energy loss than a perfect fluid. The low position of the curve may be some sort of Reynolds Number effect or it may be due to erroneous reading of the static pressure tubes, particularly those from which the working section dynamic pressure is calculated. The working section dynamic pressure is determined by taking the difference between p_o and the static pressure in the working section. Unfortunately there was not sufficient time available to check this run.

In the working section the curves are also consistent, approaching the calculated curve as the Mach Number decreases. The effect of the velocity increase through the working section at high Mach Number is clearly shown with the rate of increase becoming very much greater after $M \simeq 0.84$.

The effect of velocity decrease is still consistent in the diffuser but in addition there is another trend which is independent of the velocity. Although the lower velocity curves are approaching the calculated curve in the upstream end of the diffuser, their slopes decrease and fall much below it after a point about 25 ft. downstream from the beginning of the diffuser. This would indicate

that a considerable energy loss occurs in the diffuser between this point and the exit. The curves draw closer together toward the end of the diffuser and have almost the same value of $\frac{p-p_w}{q_w}$ at the exit, with the exception of the two highest speed runs. Both of these runs have exceeded a Mach Number of 1. They must then have suffered an energy loss in the shockwave required to restore the flow to the subsonic regime. This energy loss is reflected in the considerably lower position of the curves. The lowest speed curve is somewhat lower than would be expected. The explanation of this is probably the same as that suggested for the position of this curve in the contraction.

The main deviation of the curves from the calculated curve in the diffuser is the result of a separation in the diffuser. This result was confirmed by flow observations discussed below.

2) Velocity surveys across the entrance of the contraction.

Total head surveys across the entrance of the contraction showed a uniform velocity distribution across the entire section. Surveys were both vertically and horizontally at several air speeds. All the runs gave a constant value of total head across the section from one wall to the other.

3) Velocity survey across the working section.

It was originally planned to use the small pitot-static tube for this purpose. The instrument was calibrated at relatively

low velocities and found to read about 3% too low. The actual tests conducted with the pitot-static tube produced rather different results than were expected. These results appear in Fig. 9 . The curves show clearly that at high Mach Number the reading of the pitot-static tube is a function of the distance of the head of the tube from the wall, that is, a function of the amount of pitot tube in the tunnel. With the tube less than about 1.5 inches from the tunnel wall the error due to deflection of the tube was probably negligible. After that point the bending increased rapidly as more of the cantilever tube projected into the high velocity airstream. A calibration of the tube against angle of yaw showed a higher reading at angles up to about 15 degrees after which the reading decreased. It is believed that this yawing of the deflected tube accounts for the "hump" on the right side of the curve for Run 43. At the furthest point from the wall the pitot was yawed about 20 degrees to the tunnel centerline. It appears that the effect of increasing the amount of pitot in the tunnel tends to reduce to difference between the total head and the static reading of the pitot-static tube. Since the air compressor was a constant displacement device it is believed that the actual velocity did not change due to the presence of the pitot. The error was probably due to a variable distortion of the static reading.

These tests demonstrated that at high Mach Numbers velocity surveys must be made by instruments which do not alter the effective cross-section area as they make a traverse. The solution to the problem is to mount the head of the pitot tube on a stem that extends completely across the tunnel. In effect the pitot stem must have a dummy extending to the far side of the tunnel so that the effect of constantly changing area is removed. Such a tube was constructed for this model. Its installation required the drilling of a hole in the wall opposite the built-in pitot plug. This is somewhat difficult both because of the difficulty of accurately locating the relatively inaccessible hole, and because the hole had to be drilled in the plaster. Time did not permit the completion of this installation.

Total head readings were taken for a short distance outside the boundary layer with the boundary layer pitot. These indicate a uniform velocity profile existed at least out to .25 inch from the wall. Due to the limits of the boundary layer traverse a complete coverage of the tunnel was not possible. The total head reading outside the boundary layer agreed with the total head reading in the entrance of the contraction within 1%. Thus the loss in the contraction seems to have been small and the velocity distribution is almost certainly satisfactory. It would be expected that any energy losses would occur close to the wall. Since the loss is small at a distance as close as .1 inch from the wall, it may be assumed that the velocity profile is uniform across the section. Because of the very small curvature of the downstream portion of the contraction it is unlikely that any curvature of the streamlines exists in the working section.

4) Boundary layer surveys in the working section.

Total head surveys of the boundary layer were made at two speeds on the floor of the tunnel and checked at one of these speeds on the vertical wall. Corrections for compressibility were made to the total head readings. The profiles are shown in Fig. 10 . The results are plotted on semi-logarithmic graph paper in Fig.11 and the linear curves indicate that the boundary layer is turbulent. The curves are very similar in the three cases as would be expected. The boundary layer appears to be slightly thicker on the wall which has the greater curvature. This would be a consistent result but the effect is of the order of the experimental error. The full scale boundary layer thickness would be about 3 inches, a result which is of the correct order of magnitude.

5) Velocity surveys across the exit of the diffuser.

A total head tube mounted on a traversing arm that extended completely across the exit of the diffuser was used for this purpose. Traverses were run both horizontally and vertically. The horizontal traverses were carried out at three speeds. The profiles are shown in Fig. 12 , and in dimensionless form in Fig. 13 . The lack of symmetry indicates a separation has occurred. This separation appears to be more severe on the right side of the tunnel, looking downstream. The visual flow observations confirmed this. When plotted in dimensionless form the effect of higher velocity is

clearly shown. The separation is more pronounced for M = 0.74 than for M = 0.50. The large additional detrimental effect of a further increase in speed is shown by the curve for M = 0.90. The separation would be expected sooner with the higher velocity. It is possible that the occurrence of oblique shockwaves in the diffuser is also partially responsible for the rounded profile of the highest speed run.

The vertical traverse, shown in Figs. 14 and 15 , revealed a very severe separation on the floor of the tunnel with a definite reverse flow in this region. In an effort to locate this separation wax strips were placed at various positions in the diffuser. They did not appear to have much effect except for one placed on the floor of the tunnel upstream of the point later seen to be the separation point. The unusual affect of this wax strip was to eliminate the reverse flow at the exit as is shown in the vertical traverse plots. The velocity profile is very definitely improved and the separation much reduced. The flow of maximum velocity, however, been moved further toward the top of the tunnel so that Fig. 16 , a plot of the dynamic pressure at this station, shows little reduction in energy loss due to the wax strip. The effect of the strip seems to be due to a local separation behind the strip which draws a part of the flow closer to the lower surface and prevents the large separation from the floor.

6) Visual observations of flow in the diffuser.

The separation in the diffuser indicated by several of the above results was investigated visually. First a probe consisting

of some light tufts was used. The reverse flow, originating just about where the vertical wall runs into the cylindrical section and all the expansion is taken up by the top and bottom flat surfaces, was clearly seen. The separation seemed to occur chiefly on the floor where the rate of curvature of the floor was sharply increased. A wax fillet was built in this region in an effort to decrease the rate of expansion of the floor, and to extend this surface further downstream before it terminates in the circular section. The effect of the fillet was negligible. It was then extended further upstream but still no improvement was noticeable. The fillet may be seen in Fig. 20 .

To further investigate the flow, oil was spread over the diffuser walls for the greater part of its length. The model was then run up to speed. The flow patterns obtained were extremely instructive. The oil flowed upstream in the region which probing had indicated to be one of reverse flow. The flow was reversed over large portions of the walls, fillets, and the floor in a region much further upstream in the diffuser than was shown by the tufts. The separation originated about 30 to 35 ft. downstream from the entrance of the diffuser (full scale). This checked the results of Fig. 8 which indicate a separation in the same region. The flow patterns observed with the oil showed that separation started shortly after the diffuser broke into the 8.2 degree divergence and that the steep slope of the floor and ceiling at the end of the

diffuser merely irritated an already bad situation. This explained why the wax fillets extending the floor of the tunnel produced practically no result.

The oil flow pattern with the wax strip placed on the floor upstream of the first separation point showed a very much improved flow picture. Separation of a moderate character appeared immediately behind the strip but elsewhere the flow was always in a downstream direction. The improvement seemed just as pronounced with the oil pattern as with the probe. It will be remembered, however, that the energy gain over the duct as a whole is probably very much smaller than the improved conditions at the walls indicate.

Observations made with a screen across the exit, to simulate the resistance that the full scale diffuser will have at its exit due to the presence of the corner, produced no noticeable change in the flow pattern.

Conclusions

From the tests described above the following conclusions may be drawn.

Contraction

The entrance profile was satisfactory so that any effects observed would be due to the tunnel itself rather than to unfavorable entrance conditions. The small total head loss observed in the working section seemed to indicate that the contraction was satisfactory from the standpoint of both energy loss and velocity profile.

Working section

The boundary layer is turbulent and of the correct order of magnitude. The large increase in velocity through the working section at high Mach Numbers shows that if the tunnel is to be operated in this range some method of adjusting the walls is necessary. The only alternative is a method of continual boundary layer removal. Even with such an adjustment the Mach Number at which successful wind tunnel tests may be made is limited, however, since the model airplane's displacement area will have a large effect on the velocity of the flow in the immediate vicinity of the model. Just as small changes in areas due to the

boundary layer have large effects on the velocity, so will the changes in area due to the model have the same effect. It is difficult to see how the latter can be corrected. The practical range of Mach Numbers can possibly be increased somewhat by adjusting the walls, but probably a Mach Number of 0.85 is the upper limit for models of any reasonable size. For special experiments in which very small models are used higher Mach Numbers may be reached before the wall interference effect becomes intolerable.

Diffuser

The present diffuser has a separation at a point about one-third of its length from the entrance. It is definitely unsatisfactory. In an attempt to maintain the same end dimensions while reducing the maximum angle of divergence, another diffuser design has been suggested. It is shown in Fig. 2 . It may well be, however, that the only satisfactory solution will be to extend the length of the diffuser. To determine whether or not this will be necessary it is suggested that another model be built embodying the design of the new diffuser.

General experimental method

Application of an aerodynamic model to the problem of experimentally studying the characteristics of a high speed wind tunnel seems to have been satisfactory. Several features of the present model have demonstrated the need for improvement. As a result of this experience the following alterations in the model design are proposed.

Although the static orifices seem to have been satisfactory, it is probably desirable to reduce the size of the openings to 1/64 inch.

The static orifices should be placed along a smooth surface. Positions near a parting line should be avoided.

Traversing pitots in the high speed region should have a dummy stem so that no area change accompanies the carrying out of the traverse.

Static orifices should be spaced every inch or every 3/4 inch in the region of the working section and the first 6 inches of the diffuser.

An adjustable wall should be included in the working section to permit investigation of the practicability of correcting for the boundary layer thickness increase by similar methods in the full scale design. A design for such an adjustable wall has been developed by Mr. J. C. Schwarzenbach and has been discussed in his A.E. thesis at the California Institute of Technology, 1942.

Visual Observations of Supersonic Phenomena

Although a plate glass window was built into the roof of the working section of the model, no special visual tests were contemplated in the original experimental program. The window was included in the model design chiefly to allow easy alignment of the velocity measuring instruments placed in the working section at various times, and to permit observation of possible excessive vibration or other disturbances of the pitot-static or total head tubes. During the first few runs it was noticed that a small quantity of oil was present in the air. This oil originated in the compressor and apparently penetrated the oil filters. At first considered an objectionable characteristic of the system, the oil proved to be a means of visually observing local shock waves occurring in the working section because of the interference of the pitot static tube.

The initial observations of the oil flow showed that the oil, being of rather high viscosity, moved slowly along the floor and roof of the working section following the streamlines of the air flow. It would, of course, be expected that the slowly moving oil would be moved only by viscous interaction with the air and would follow the path of the adjacent airstream. Introduction of the pitot-static tube through the floor of the tunnel produced the equivalent of a two-dimensional circular cylinder, namely the stem of the tube, in the lower region of the working section. The oil stream pattern on the floor of the tunnel in the region of the tube at low velocities was similar to that of potential flow around such a cylindrical body. The wake behind the stem formed just as would be

expected behind a bluff body. As the Mach Number in the working section approached 0.7, the pattern behind the pitot stem assumed a wedged shaped or triangular character, the apex of the triangle being just at the rear surface of the stem. This wedge line appeared to form a barrier past which most of the oil would not pass. Since this line was very close behind the pitot stem and in its immediate wake, the oil, after reaching the barrier, reversed its flow direction and traveled toward the pitot, apparently piling up into a small globule. It then appeared to flow back into the stream, either passing downstream beyond the small wedge, or else repeating its vortex-like path behind the stem. The wedge barriers were at an angle of about 45 degrees to the freestream velocity. Their length at this stage was about one diameter of the stem. It will be noted that the pitot stem has a diameter of about .05 inches while the width of the tunnel is close to 3.1 inches at this station.

Increase of velocity until a Mach Number of .9 was reached caused a gradual widening of the barriers described above. Their form changed somewhat in that as they extended further from the immediate region of the stem, and away from the wake, they became thicker and stronger. At the highest speed the two barriers trailed behind the stem at an angle of about 45 degrees from the freestream flow direction, started about one-eighth inch from the pitot and had a length of the order of a quarter inch. Instead of just a small line, a considerable accumulation of oil appeared, giving the oil

patch a thickness of approximately one-sixteenth inch. The faster portion of the flowing fluid passed through the oil patches but most of the fluid did not appear to have had the energy to do so. Instead it traveled tangent to the oil patches in the direction leading downstream and to the side, and away from the pitot stem, and after reaching the end of the oil patches flowed straight downstream again. The small initial barriers close to the pitot remained but appeared very small compared to the larger oil patches.

The nature of this phenomenon appears to clearly indicate the presence of shockwaves caused by local supersonic velocities in the region of the pitot stem. The freestream Mach Number was approximately .7 to .9 in the speed range at which the flow irregularities appeared. Thus the velocity in the potential field affected by the cylindrical stem would be expected to become greater than that of sound. It has been shown that sonic velocity occurs at the point of maximum thickness of a cylinder when the freestream Mach Number is 0.42 . With greater Mach Numbers sonic velocity is reached upstream of the maximum thickness point. Downstream of the sonic velocity region the streamlines diverge and the flow near the cylinder becomes supersonic. The flow far from the pitot is subsonic in the working section at all times so that the small region of supersonic velocity cannot be expected to continue very far. A

shockwave then occurs. It is visually observable because the slow moving viscous oil does not have the kinetic energy to carry it against the adverse pressure drop occurring at the shock where the low pressure in the supersonic region on the upstream side is raised to a higher pressure present in the subsonic flow on the downstream side of the shockwave.

In order to improve the visibility of the shock, oil in larger quantities was introduced into the large section upstream of the contraction. At first too light an oil was used. The rapid flow of the fluid allowed it to pass through the pressure drop and washed away the oil patches. Use of a more viscous oil improved the entire flow pattern of the oil. This result seems to confirm the explanation of this phenomenon given above.

Additional observations of this high speed effect were made through the open end of the diffuser. Due to the high velocity at the exit it is necessary to stand at least eight to ten feet from the end of the diffuser. At this distance the jet is sufficiently diffused to allow sustained observation of the section of the tunnel from the working section to the end of the diffuser. At high speeds a sort of halo was first observed around the pitot-static tube placed, as in the above discussion, on the floor of the working section. Additional systematic observations were made both with and without the pitot in the tunnel, and at various air speeds. The results are of considerable interest and appear to be definitely related to

the occurrence of shockwaves both in the vicinity of the pitot and in the diffuser.

At the maximum velocity, Mach Number = 0.9, the view through the exit end of the diffuser in the direction of the pitot revealed a canopy shaped pattern of haze surrounding the pitot tube. The thickness of the layer of haze perpendicular to the centerline of the tunnel was small, probably of the order of a sixteenth of an inch. The layer was parallel to the stem of the pitot and about one-half inch from it along the sides. The top layer was an arc, almost circular, joining the sides and passing just above the top of the pitot stem. The lower layer warped in toward the centerline from the side layers similar to the top arc, but since the pitot does not end in the airspace on the bottom as at the top but passes through the floor, the lower arc strikes the floor some distance from the center of the tunnel. It appears that the intersection of the lower arc and the floor is just about as far from the centerline of the tunnel as the outer extremities of the oil patches described above. Shifting the point of view slightly off the centerline showed that this canopy extends downstream at least six to eight inches. Whether it then disappeared or merely became difficult to see due to lessened contrast with the color of the walls in that section could not be definitely determined.

With decreased velocity the canopy gets narrower, shrinking closer to the pitot, but retaining the same general character.

When the sides of the canopy have closed in to within about a quarter inch of the pitot stem the pattern becomes somewhat unsteady with portions of the sides vibrating laterally with an irregular period. At a Mach Number of about .75 the sides of the canopy moved so close to the center that they lost their separate identity and appeared as a wider vertical strip of haze behind the pitot. Correlation between the decreasing distance of the sides from the pitot and the decreasing length of the oil patches was noted. The small wedge shaped oil pattern behind the pitot seemed to coincide with the appearance of the vertical strip of haze. At still lower velocity the haze disappeared completely.

The above discussion is related to supersonic velocities arising in the velocity field of the pitot tube stem. Since the main flow also became supersonic at the beginning of the diffuser it is clear that some sort of shock must occur in this region. This main transition shockwave is also visible in that it causes a condensation similar to that described above but with less definite form. With the tunnel clear, that is with the pitot removed from the working section, no haze is noticeable in the working section or the diffuser at subsonic velocities. Coincident with the reaching of sonic velocity at the end of the working section a very definite white haze appears to extend all across the tunnel near the beginning of the diffuser. The haze is quite uniform in color across the section but exhibits rapid irregular fluctuations. With increasing velocity the fluctuations die out, and the haze becomes less pronounced.

At the highest velocity a steady light mist with a definite irregular pattern exists. The haze seemed to extend completely across the section with some clear patches which look like dark spots on the white background. One of the dark spots is oval shaped and extends down from the roof of the tunnel. The other major spots are generally circular and are unsymmetrically placed across the section.

Superimposing the effects of the pitot tube on the major shock (by replacing the pitot in the working section) resulted in a pattern exactly like the one just described, but with the very much more distinct canopy passing through the haze of the major shock. A striking effect, however, is that the region under the canopy is completely clear whereas without the pitot and its canopy this area would be hazy.

It might also be noted that the boundary layer region within a few millimeters of the wall was at all times clear of any indication of condensation. The lower velocities in the boundary layer easily explain this.

It would seem that the canopy is essentially a surface of condensation of either water or oil. The exact nature of such a condensation and the particular reason for its appearing at the edge of the shockwave is not entirely clear. It is known of course that large pressure and temperature changes occur in the high speed region and across the shockwave. In the supersonic region the low temperature tends to condense the evaporated liquid while the low pressure opposes this effect. Downstream of the shockwave an increased temperature tends

to prevent condensation while the higher pressure encourages it. These opposing effects must be balanced against the vapor pressure curve for the water or oil vapor present in the airstream, and against the initial pressure and temperature conditions of the air. It appears from the observations described above that just at the outer edges of the local shockwave behind the pitot tube the pressure temperature curve of the air crosses the vapor pressure and temperature curve for the vapor present in the air. Therefore condensation occurs along the edges of the shockwave, and the condensed vapor then flows downstream with the air streamlines. That the condensed vapor passes without further change through the main transition shock in the diffuser may seem somewhat remarkable, but the observations show clearly that this is so. It is difficult to see why this condensation should occur only at the edges of the shockwave surface while no traces of condensation are visible anywhere else in the region of the local pitot shockwaves. Possibly careful measurement of the degree of saturation of the air, and calculation of the velocity and pressure fields in the vicinity of the pitot and the shockwave would reveal a precise explanation.

When we consider the transition shock in the diffuser we find that a very definite condensation effect is produced with the Mach Number just over the value of one. The nature of the pattern indicated that this first shock may be a straight shock. As the speed increased the haziness decreased, and the visible pattern looked more like a series of oblique shocks. There may be a significance in

that the greatest haze occurred when the shock took place with a Mach Number close to 1, and that the haze decreased at higher Mach Numbers. This is in agreement with the finding at the local pitot shock where the region of condensation was at the border of the shock, that is in the region where the Mach Number is also just about equal to 1.

The lack of condensation under the canopy behind the pitot even after passing through the transition shock which filled the rest of the channel with haze indicates that the temperature increase accompanying the local shock was sufficient to prevent condensation at the second shock. Such a conjecture is not unreasonable since the consistent appearance of the haze in its strongest form in regions of close to sonic velocity would seem to show that the conditions for the appearance of the phenomenon are quite restricted, and that therefore the change introduced by the first shock would cause a large enough disturbance of these conditions to forestall further condensation. Thus it may be that the temperature and pressure changes accompanying sonic velocity tend to cause condensation, but that if the velocity substantially exceeds sound velocity the resulting shock is of sufficient strength to increase the temperature and prevent condensation.

Some correlation between higher humidity in the free air and greater density of the haze patterns was noted, and leads to the belief that the haze may have consisted of condensed water rather than oil. This is far from conclusive, however, since the evidence is based only upon the observers' opinion.

References

1. Ackeret, J., "Windkanalle fuer Hohe Geschwindigkeiten." Convegno di Scienze, Matematiche, e Naturali, Rome, 1936

2. Glauert, H., "The Elements of Aerofoil and Airscrew Theory", Cambridge University Press, London, 1937

3. Th. von Karman, "Compressibility Effects in Aerodynamics", Journal of the Aeronautical Sciences, 1941, Vol. 8, No. 9, p. 337

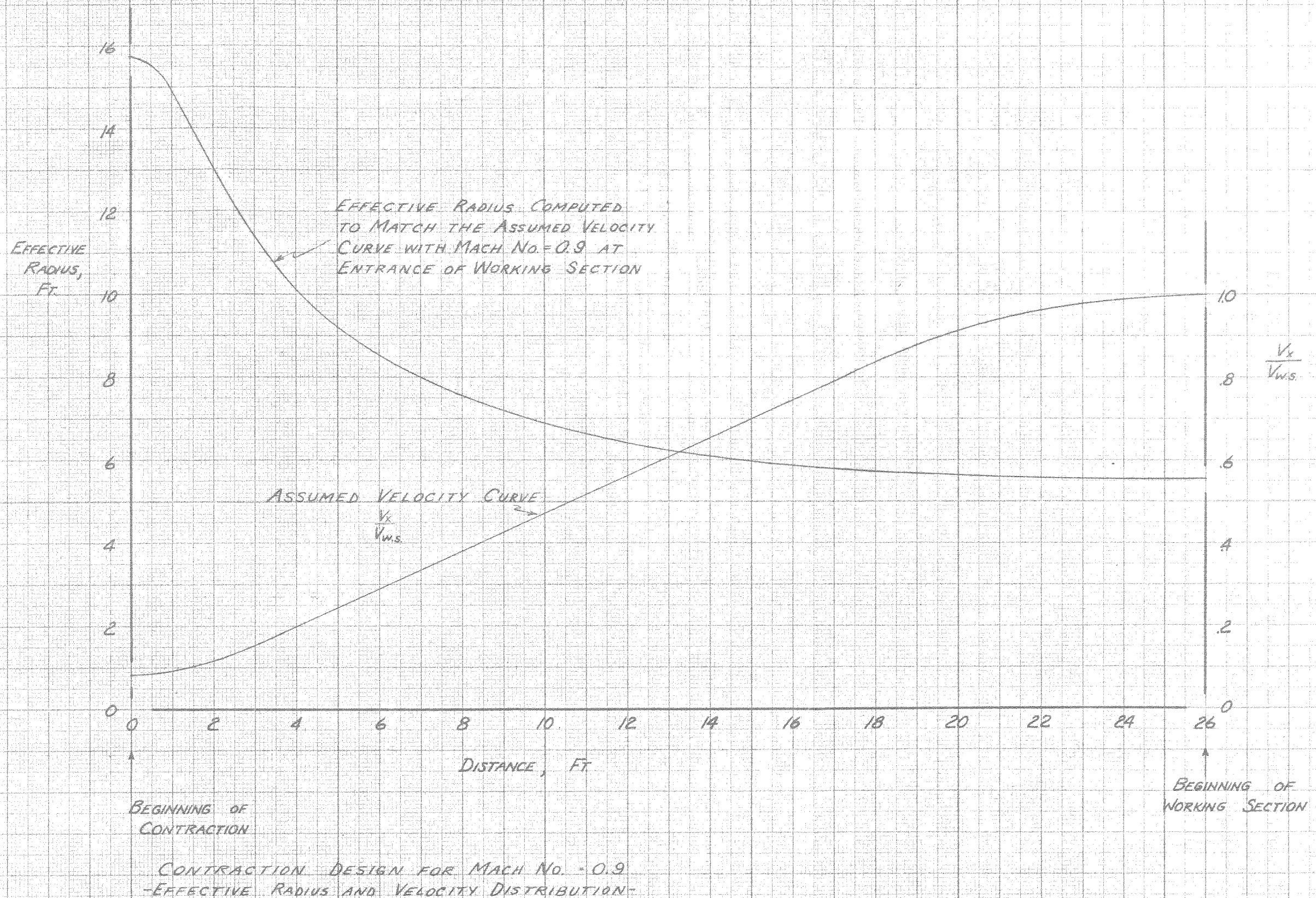

CONTRACTION DESIGN FOR MACH NO. = 0.9
-EFFECTIVE RADIUS AND VELOCITY DISTRIBUTION-

Shevell-vs-1942

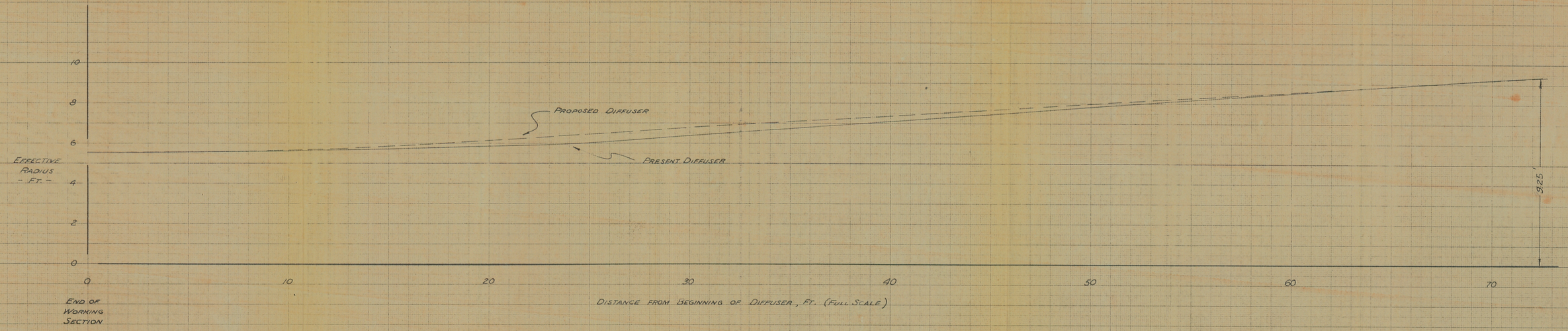

PROPOSED AND PRESENT DIFFUSER DESIGNS FOR
COOPERATIVE WIND TUNNEL
— EFFECTIVE RADIUS —

Shevell-rs-1942

ASSEMBLY

1½"=1'-0"

SCREENS

8" STD. PIPE MACHINE TO 8⅛ I.D.

AIR

⅜/16

10"

26"

58½" APPROX.

L 2½"x2½"x⅜/16

COMPRESSOR TANK

8" STD. WELDING NECK

8" STD. GATE VALVE

4½"

GASKETS

SCREENS

TOP

.501"

6.708" (22'-0")

4.644" (18'-0")

18.834" (73'-0")

2.25" 1.562" 1.16" .91" .73" .606" .418" .28" .183" .124" .0858" .0432" .0268" .0163" .0109" 0"

.0109" .0163" .0268" .0432" .0858" .124" .183" .28" .418" .606" .73" .91" 1.16" 1.562" 2.25"

.0101" .0215" .062" .102" .167" .215" .316" .382" .452" .527" .684" .899" 1.14" 1.288"

31'-6" I.D. OR 8⅛" I.D.

1.097"

.475 REF.

.776" REF.

A

B

D

GLASS

PROJECTION

AIR

0' 1.84' 3' 4' 5' 6' 8' 10' 12' 14' 16' 18' 20' 22' 24' 26'

0' 10' 10' 15' 20' 25' 30' 35' 40' 45' 50' 55' 57.5' 60' 65' 70' 73'

1.290" REF.

FOR DIMENSIONS SEE DWG. 5-266-130

FOR DIMENSIONS SEE DWG. 5-266-130

WOOD

L 2"x2"x3/16

ELEVATION

AIR DUCT SCALE: 0.258"=1'-0"

REFERENCE DWG. 5-266-129 & 5-266-130

MATERIAL	FINISH	HEAT TREAT	DRAFTSMAN	CHECKED	APPROVED	ENGINEER
			F.U. 3-20-42			

TOLERANCES ± .010 OR ± UNLESS OTHERWISE NOTED

SCALE: FULL SIZE

GUGGENHEIM AERONAUTICAL LABORATORY
CALIFORNIA INSTITUTE OF TECHNOLOGY

COOPERATIVE WIND TUNNEL
AERODYNAMIC MODEL
NAME

5-266-128
DRAWING NO.

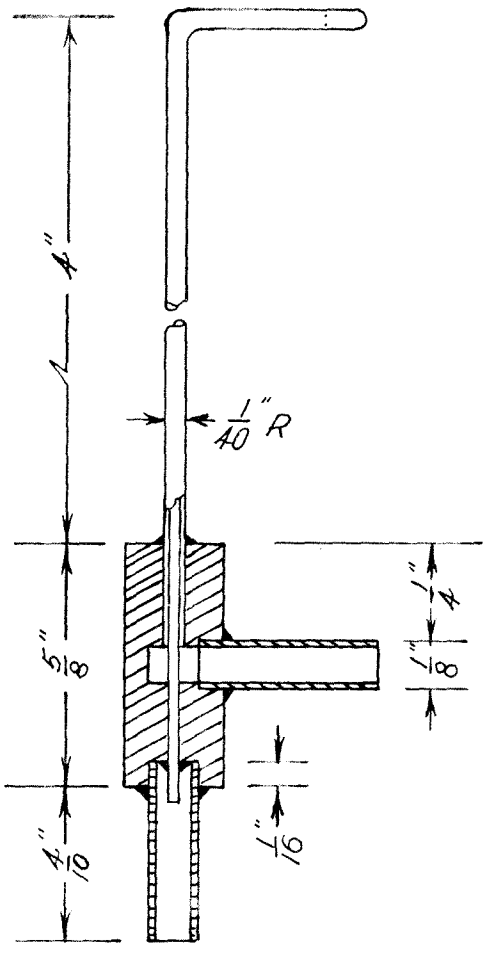

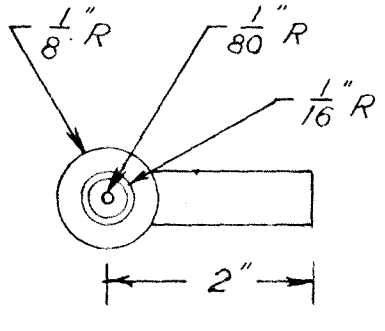

▲ SOLDER

SCALE: 1" = 2"

12' CO-OPERATIVE WIND TUNNEL
AERODYNAMIC MODEL
PITOT-STATIC TUBE OUTLET PLUG

RSS:HM

M = LOCAL MACH NUMBER
P = LOCAL PRESSURE
P_0 = STAGNATION PRESSURE

M

1.1
1.0
.9
.8
.7
.6
.5
.4
.3
.2
.1
0

0 .1 .2 .3 .4 .5 .6 .7 .8 .9 1.0

P/P_0

CURVE OF P/P_0 VS MACH NUMBER

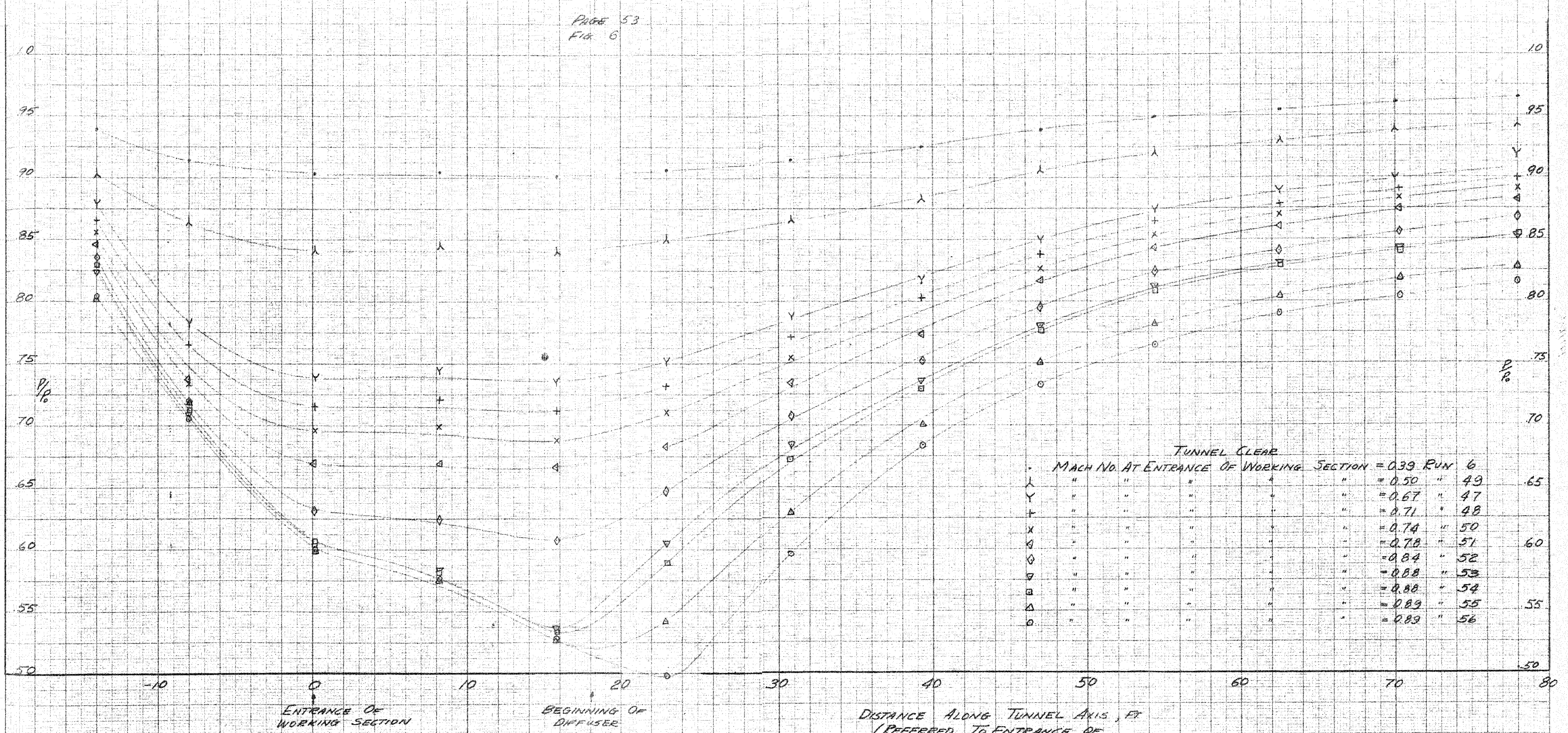

VARIATION OF p/p_0 IN THE CONTRACTION, WORKING SECTION, AND DIFFUSER FOR VARIOUS MACH NUMBERS AT THE ENTRANCE OF THE WORKING SECTION

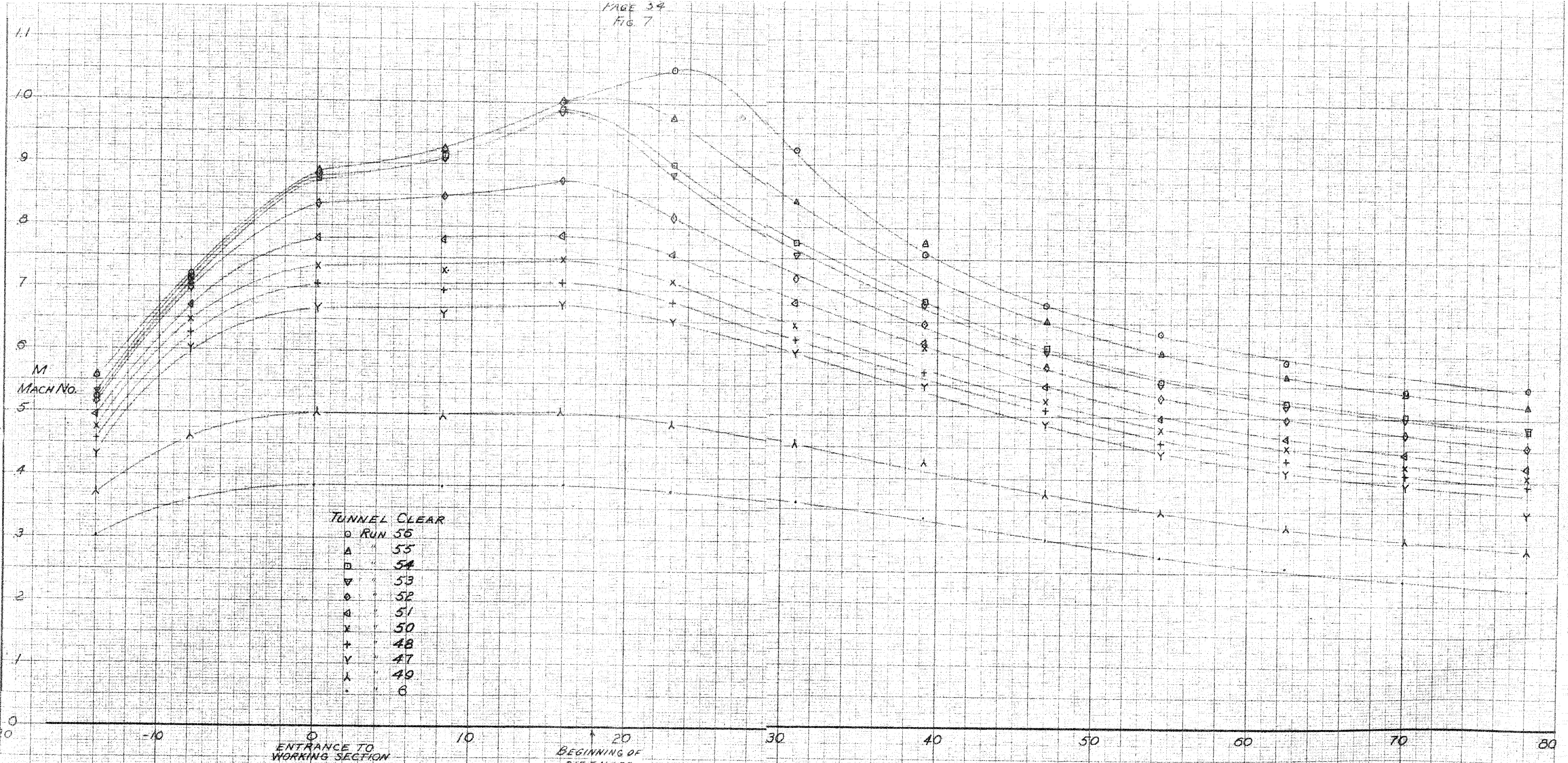

MACH NUMBER VARIATION IN THE CONTRACTION, WORKING SECTION, AND DIFFUSER FOR VARIOUS MACH NUMBERS AT THE ENTRANCE OF THE WORKING SECTION

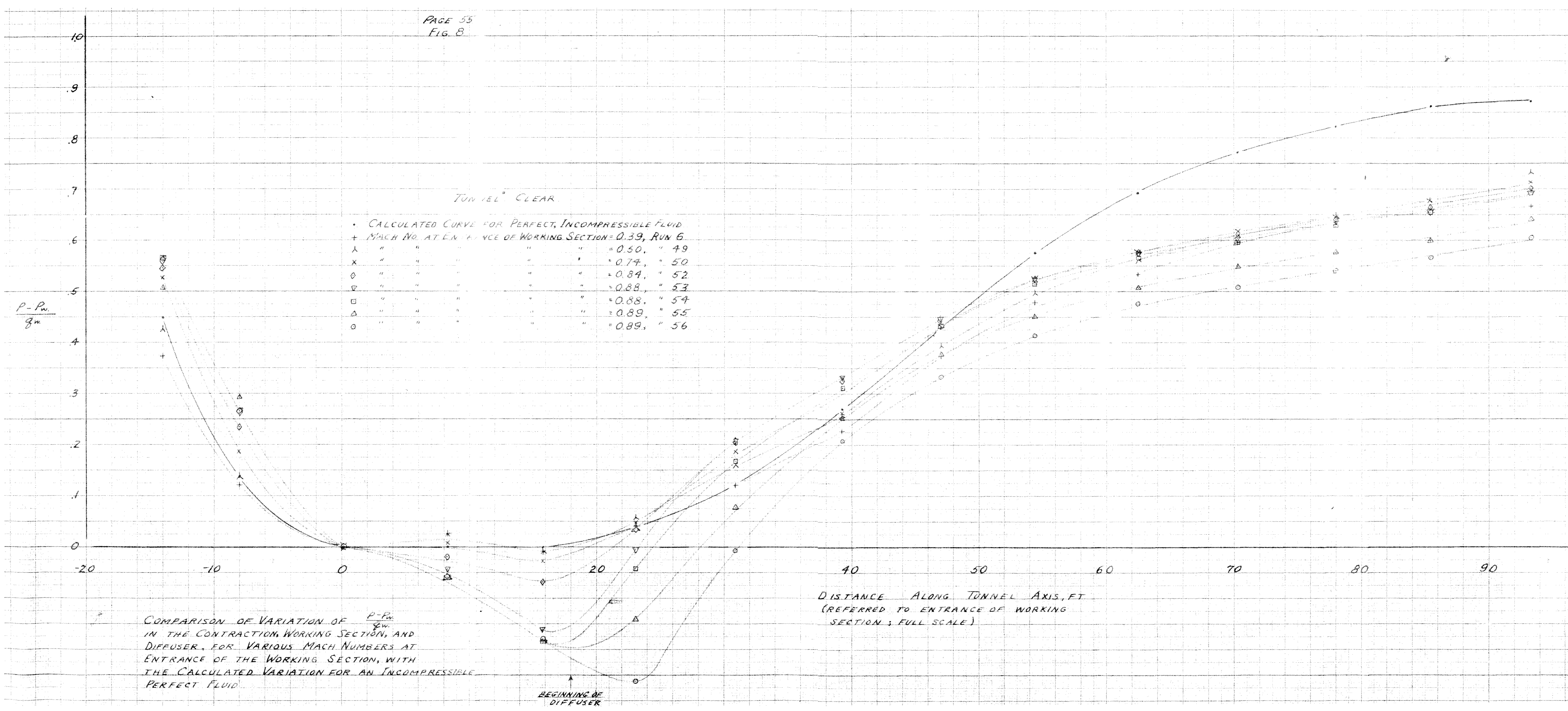

COMPARISON OF VARIATION OF $\frac{P-P_w}{q_w}$ IN THE CONTRACTION, WORKING SECTION, AND DIFFUSER, FOR VARIOUS MACH NUMBERS AT ENTRANCE OF THE WORKING SECTION, WITH THE CALCULATED VARIATION FOR AN INCOMPRESSIBLE PERFECT FLUID

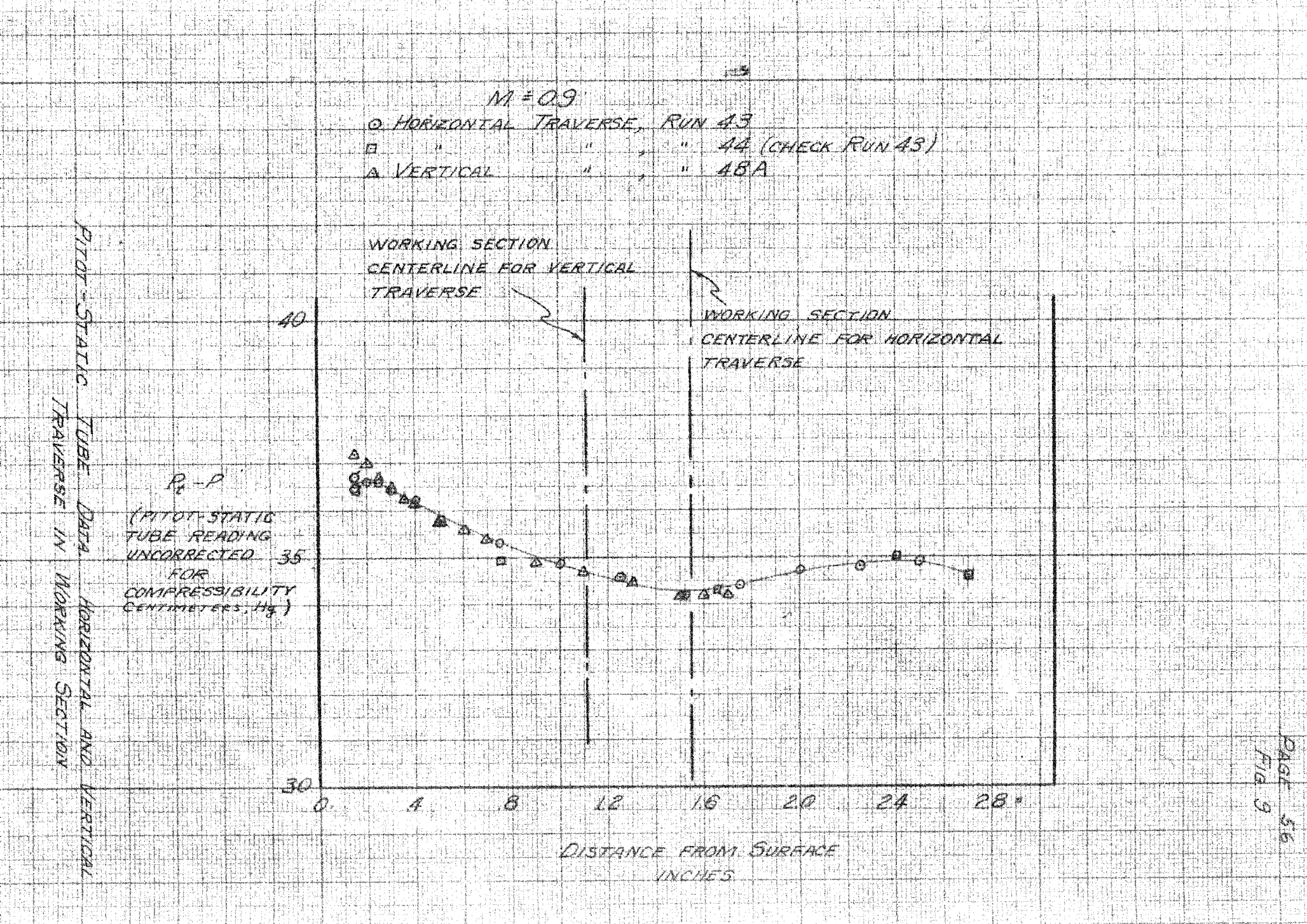
M = 0.9
○ HORIZONTAL TRAVERSE, RUN 43
□ " " " 44 (CHECK RUN 43)
△ VERTICAL " " " 48A
WORKING SECTION CENTERLINE FOR VERTICAL TRAVERSE
WORKING SECTION CENTERLINE FOR HORIZONTAL TRAVERSE
$P_t - P$
(PITOT-STATIC TUBE READING UNCORRECTED FOR COMPRESSIBILITY CENTIMETERS, Hg)
40
35
30
0
4
8
12
16
20
24
28"
DISTANCE FROM SURFACE INCHES
PITOT-STATIC TUBE DATA. HORIZONTAL AND VERTICAL TRAVERSE IN WORKING SECTION

PAGE 56
FIG 9

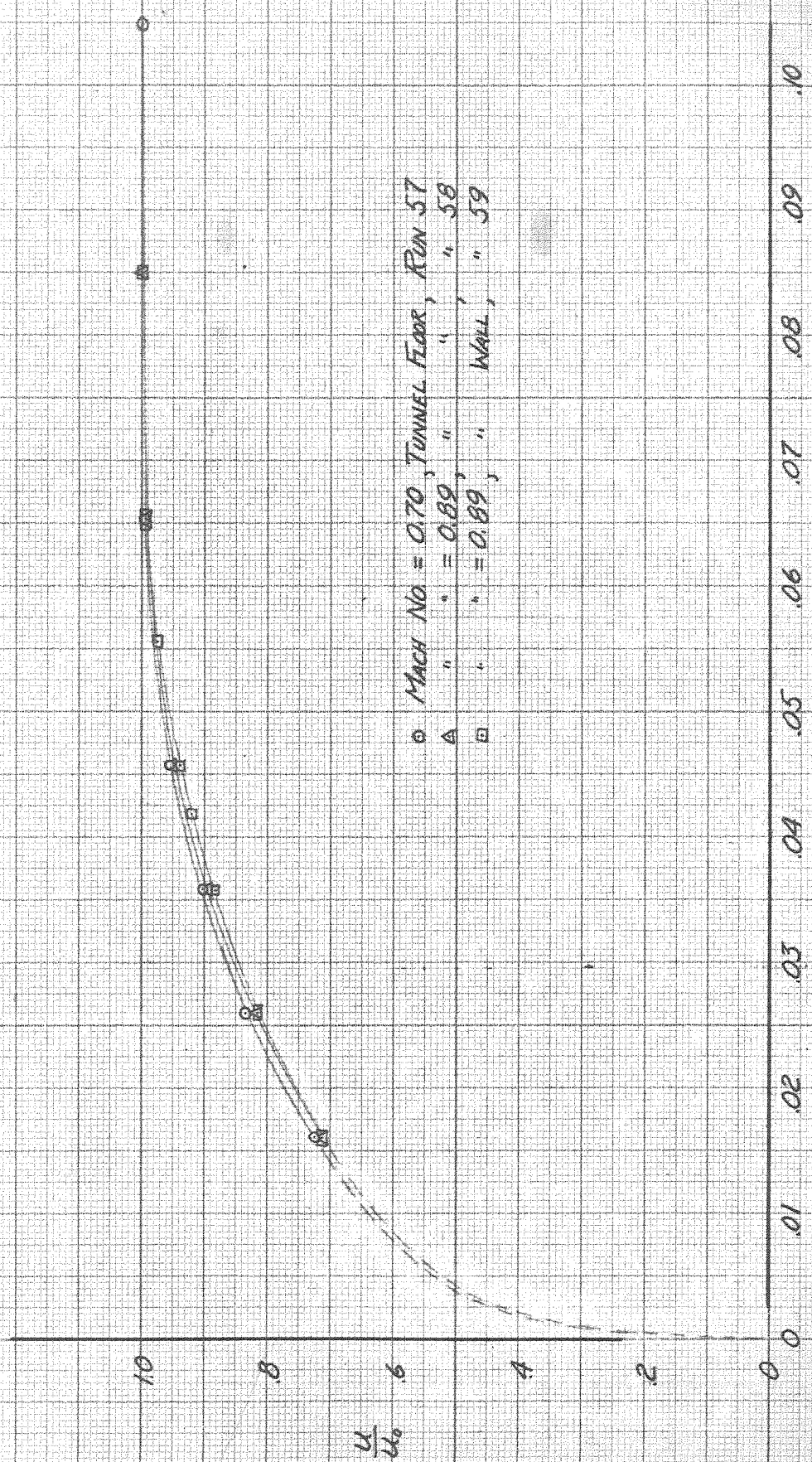

BOUNDARY LAYER PROFILES AT STATION .046" BACK FROM ENTRANCE TO WORKING SECTION (MODEL SCALE)

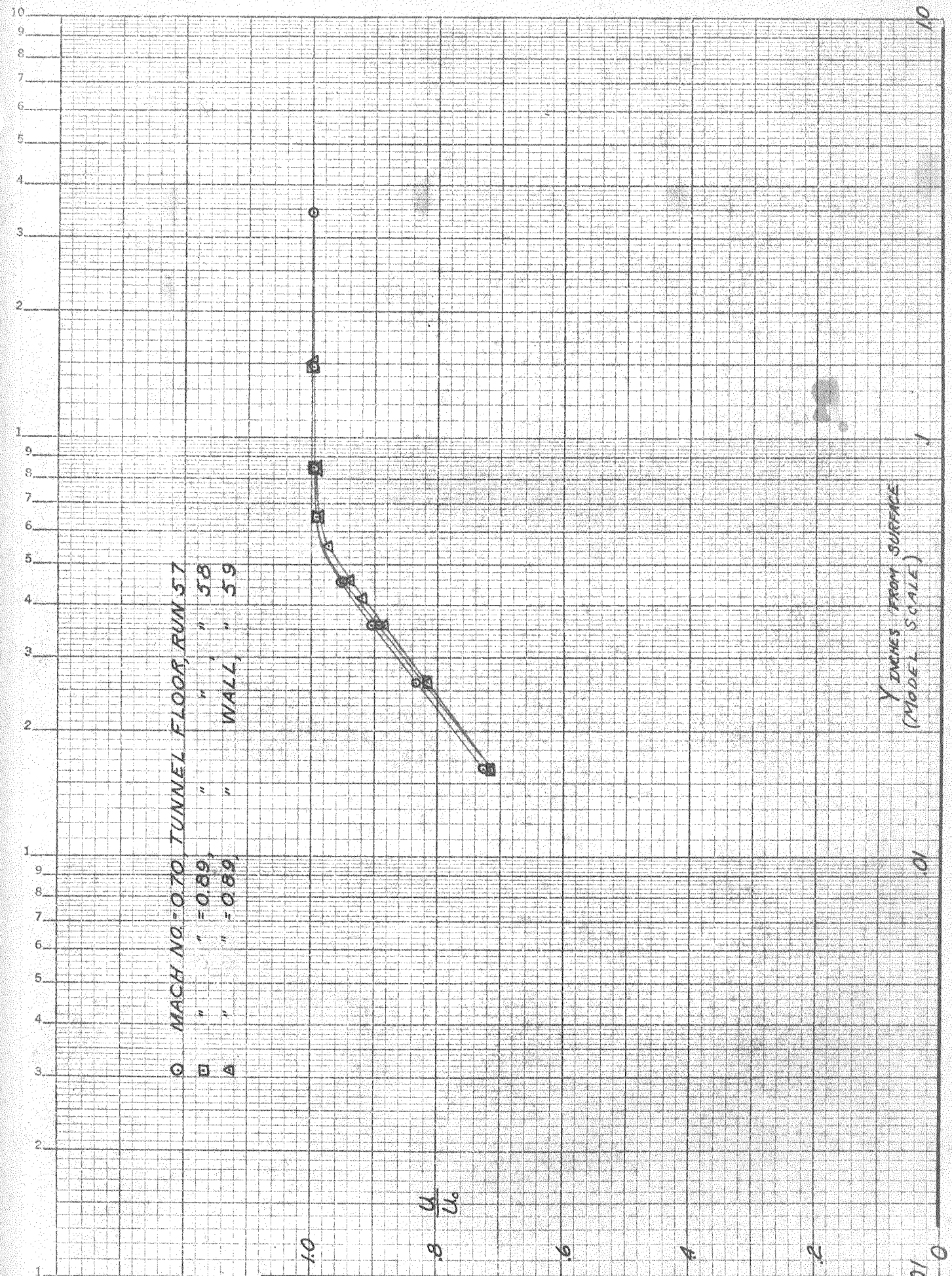

LOGARITHMIC BOUNDARY LAYER CURVE FOR STATION .046" BACK FROM ENTRANCE TO WORKING SECTION (MODEL SCALE)

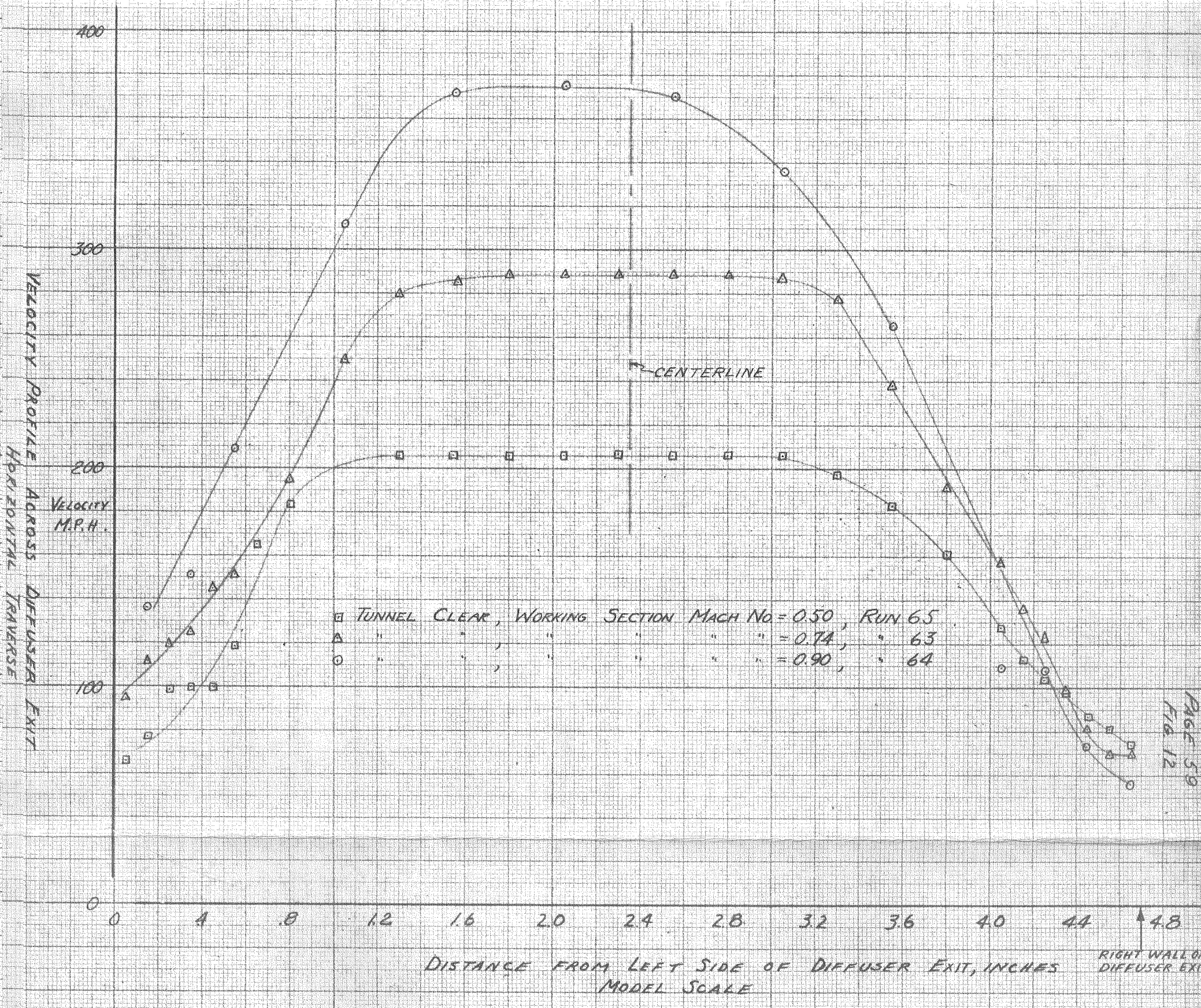
400
300
200
100
0
VELOCITY M.P.H.
VELOCITY PROFILE ACROSS DIFFUSER EXIT
HORIZONTAL TRAVERSE
CENTERLINE
TUNNEL CLEAR, WORKING SECTION MACH NO = 0.50, RUN 65
" " " " " = 0.74, " 63
" " " " " = 0.90, " 64
0
.4
.8
1.2
1.6
2.0
2.4
2.8
3.2
3.6
4.0
4.4
4.8
DISTANCE FROM LEFT SIDE OF DIFFUSER EXIT, INCHES
MODEL SCALE
RIGHT WALL O
DIFFUSER EX
FIG 12

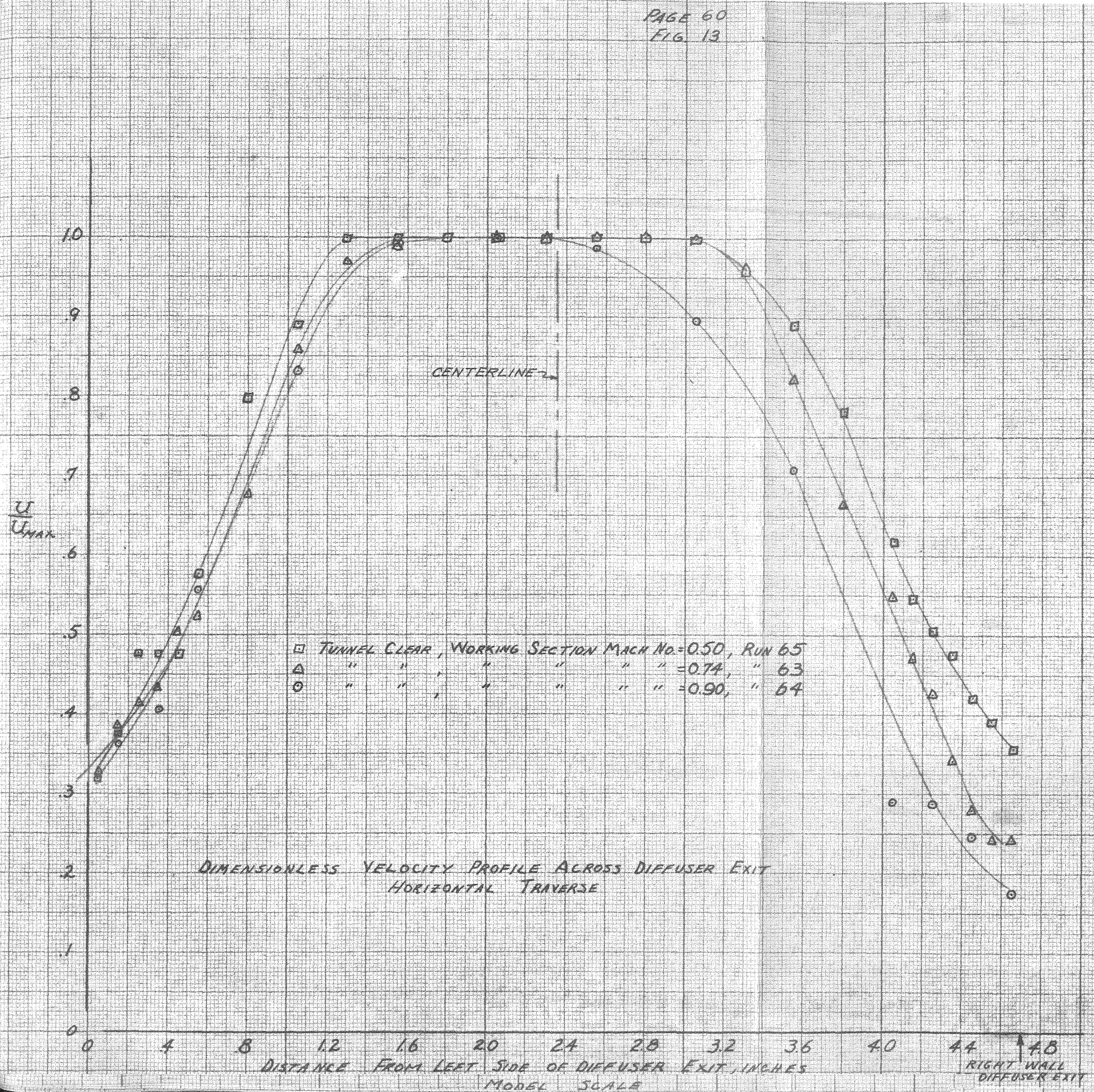
1.0
.9
.8
.7
.6
.5
.4
.3
.2
.1
0
U/U MAX.
CENTERLINE
0
.4
.8
1.2
1.6
2.0
2.4
2.8
3.2
3.6
4.0
4.4
4.8
RIGHT WALL DIFFUSER EXIT
□ TUNNEL CLEAR, WORKING SECTION MACH NO. = 0.50, RUN 65
△ " " , " " " " = 0.74, " 63
⊙ " " , " " " " = 0.90, " 64
DIMENSIONLESS VELOCITY PROFILE ACROSS DIFFUSER EXIT
HORIZONTAL TRAVERSE
DISTANCE FROM LEFT SIDE OF DIFFUSER EXIT, INCHES
MODEL SCALE

MACH. NO. (WORKING SECTION) = 0.5

⊙ TUNNEL CLEAR , RUN 66

△ WAX STRIP, 0.15" HIGH, 0.25" WIDE, " 67
EXTENDS FROM LEFT LOWER
FILLET TO RIGHT LOWER FILLET
ACROSS TUNNEL FLOOR ABOUT
15 FT. (FULL SCALE) DOWNSTREAM
FROM WORKING SECTION ENTRANCE

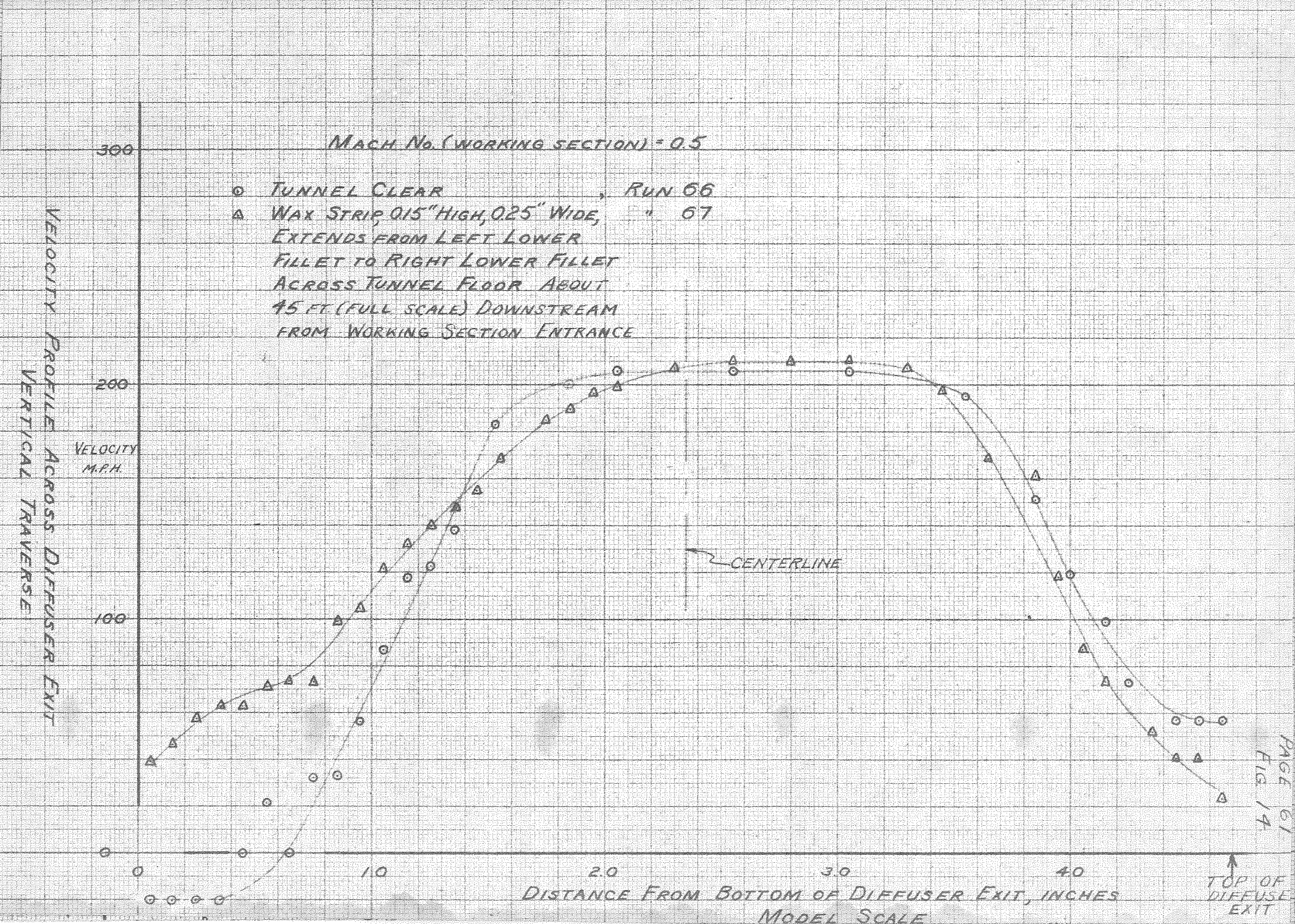

PAGE 61
FIG 14

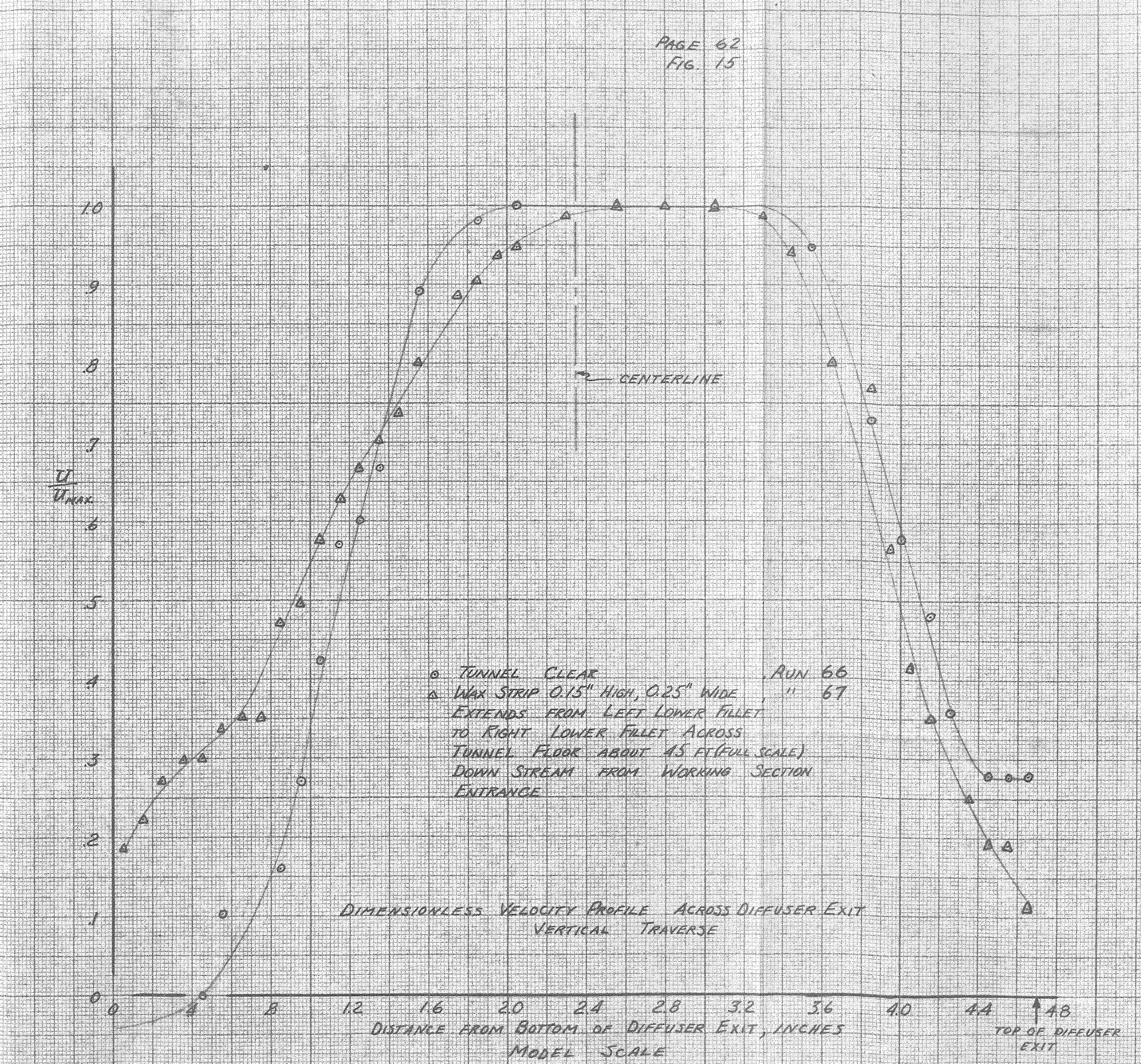

DIMENSIONLESS VELOCITY PROFILE ACROSS DIFFUSER EXIT
VERTICAL TRAVERSE

DISTANCE FROM BOTTOM OF DIFFUSER EXIT, INCHES
MODEL SCALE

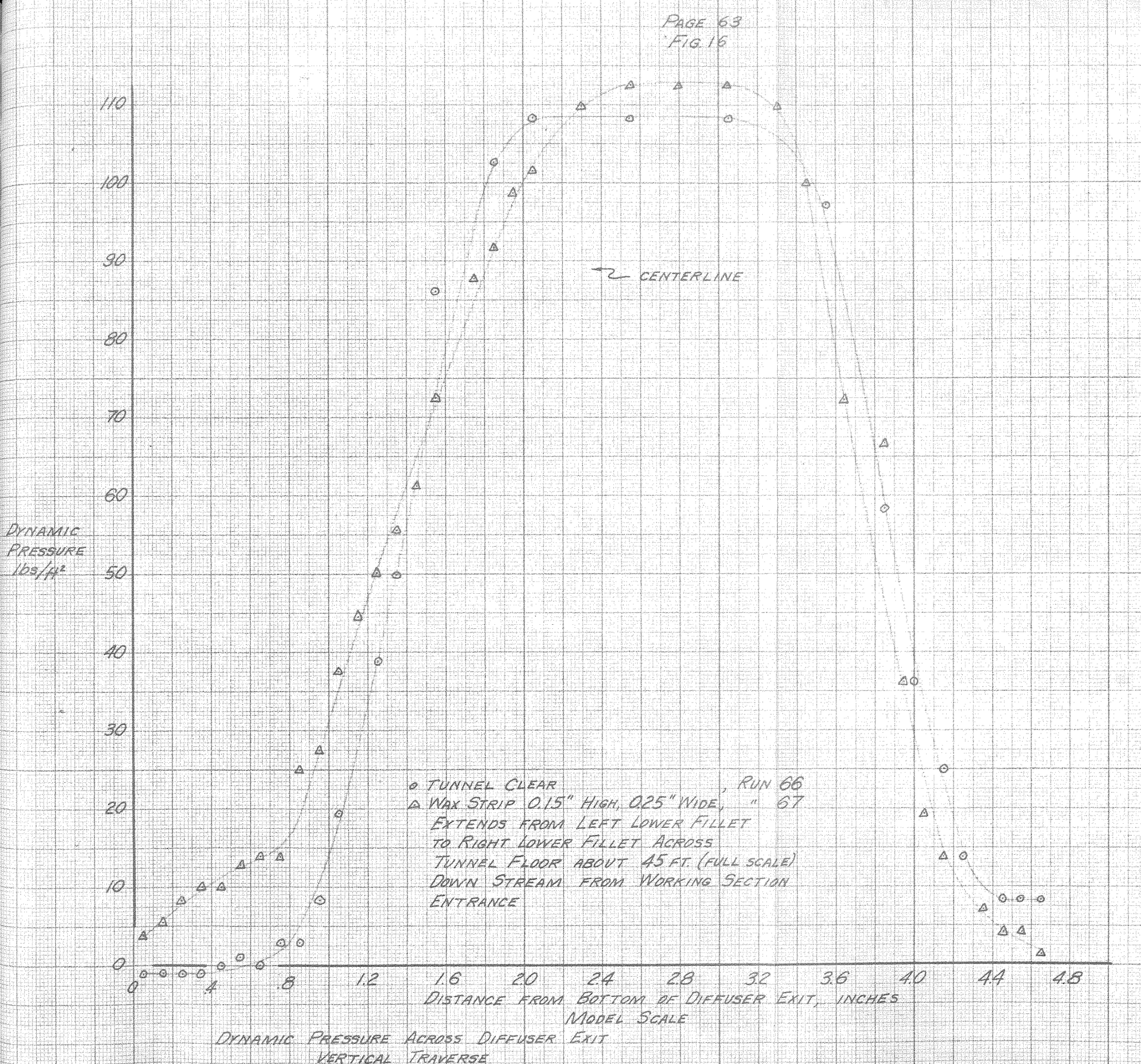

DYNAMIC PRESSURE ACROSS DIFFUSER EXIT
VERTICAL TRAVERSE

Fig.17-Upper half of Pattern of Aerodynamic Model

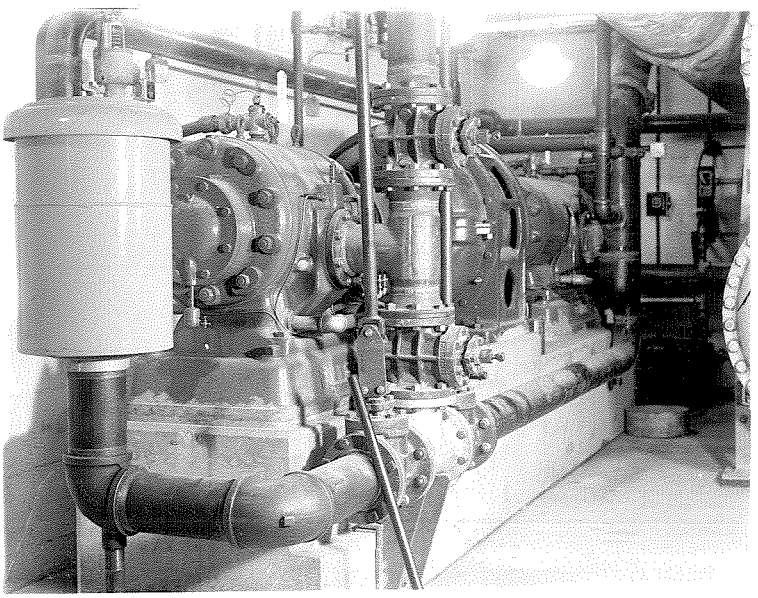

Fig.18-Air Compressor Equipment

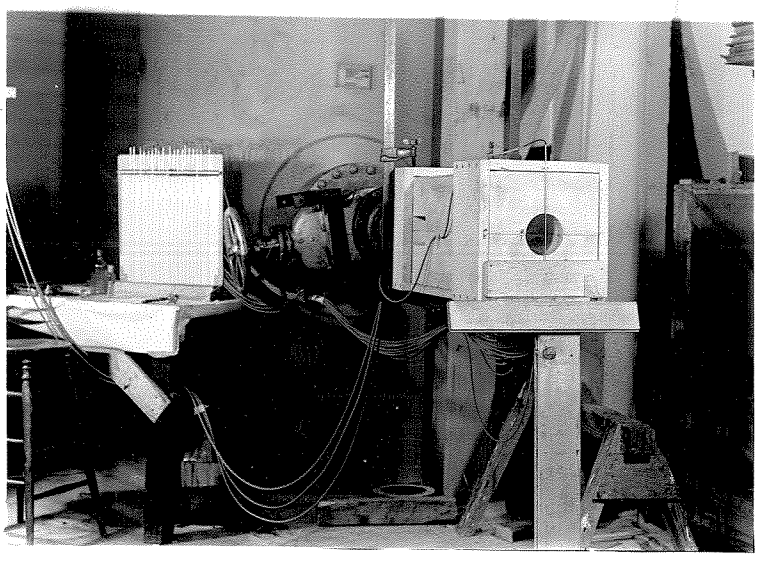

Fig.19-General View of Test Set-up Showing Model and Multiple Manometer.Traversing arm is in position at diffuser exit.

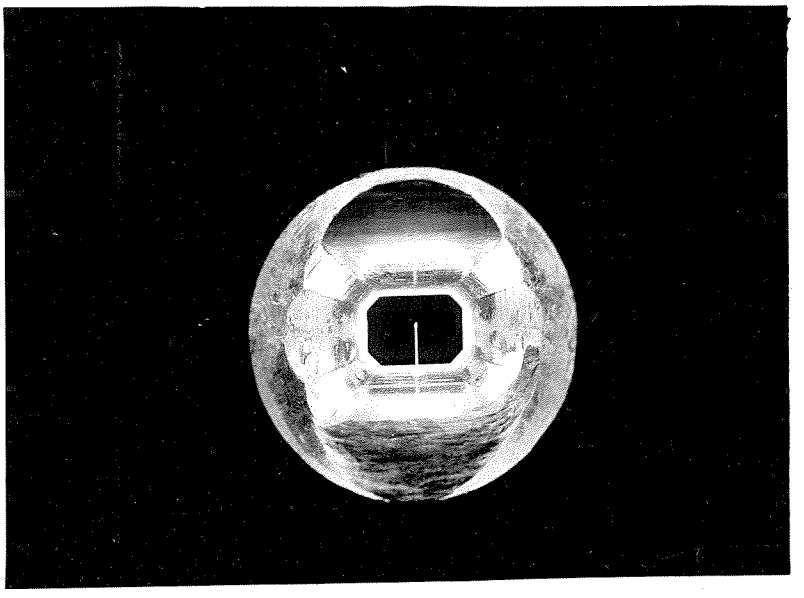

Fig.20-View of Diffuser Looking from the Exit toward the Working Section.Wax fillet is on the floor near the exit.Pitot-static tube is installed in the working section.

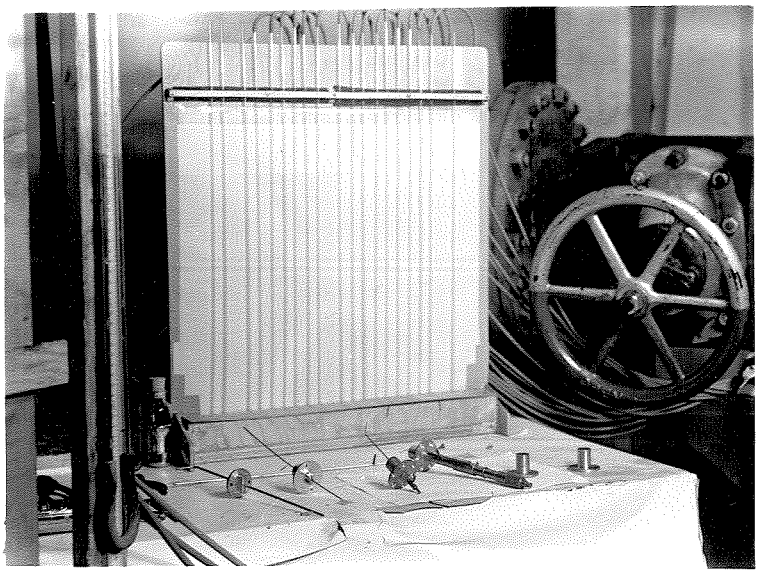

Fig.21-Multiple Manometer, Total Head Tubes, Pitot-static tube, and Boundary Layer Survey Instrument.

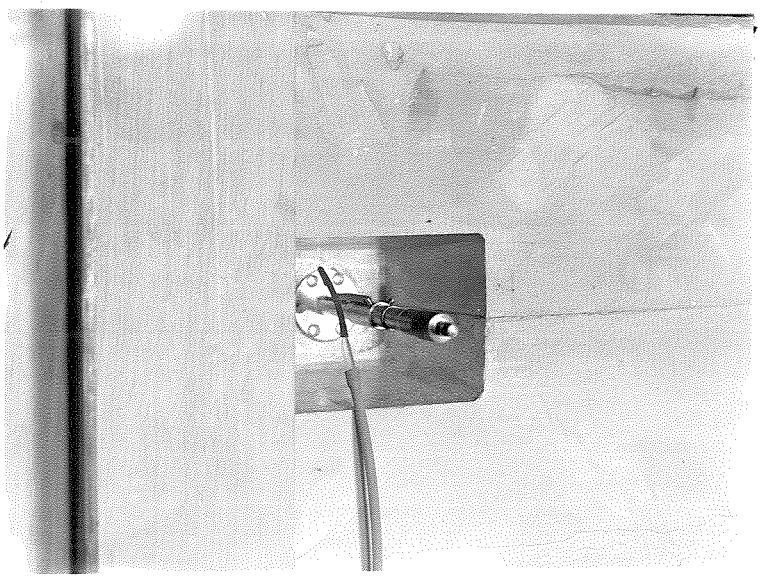

Fig.22-Close-up of Micrometer Head of Boundary Layer Survey Instrument Installed in Tunnel Wall.

(see page 38)

All photographs taken through exit end of the diffuser.

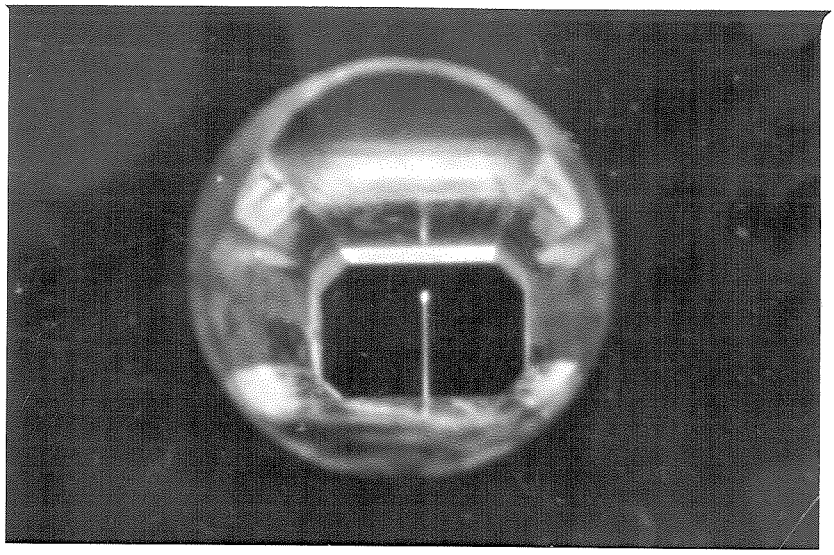

Fig. 23 - Speed below critical velocity for pitot halo.

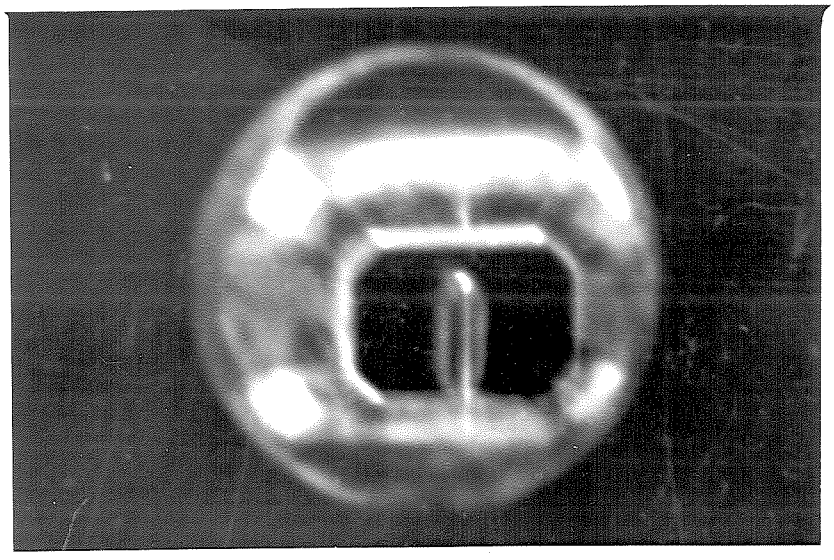

Fig. 24 - Speed slightly higher than that at which pitot halo first appears.

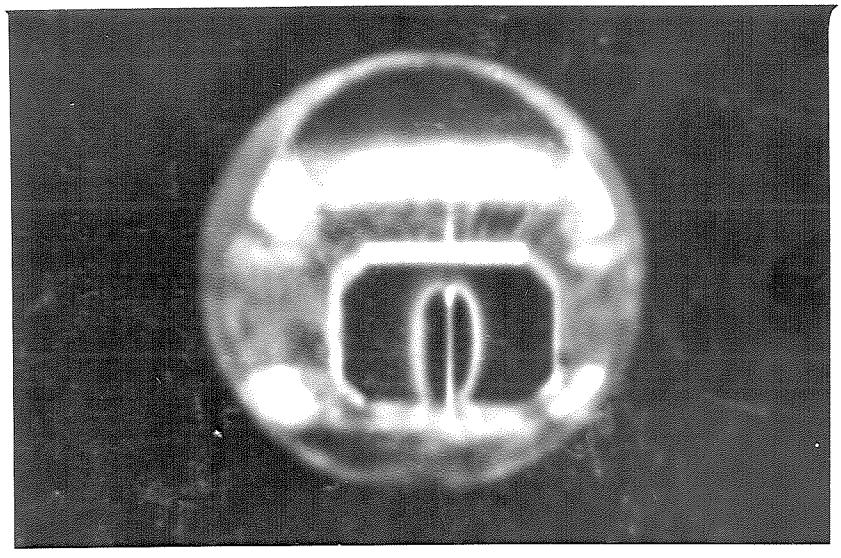

Fig. 25 - Intermediate speed. No haze outside of halo.

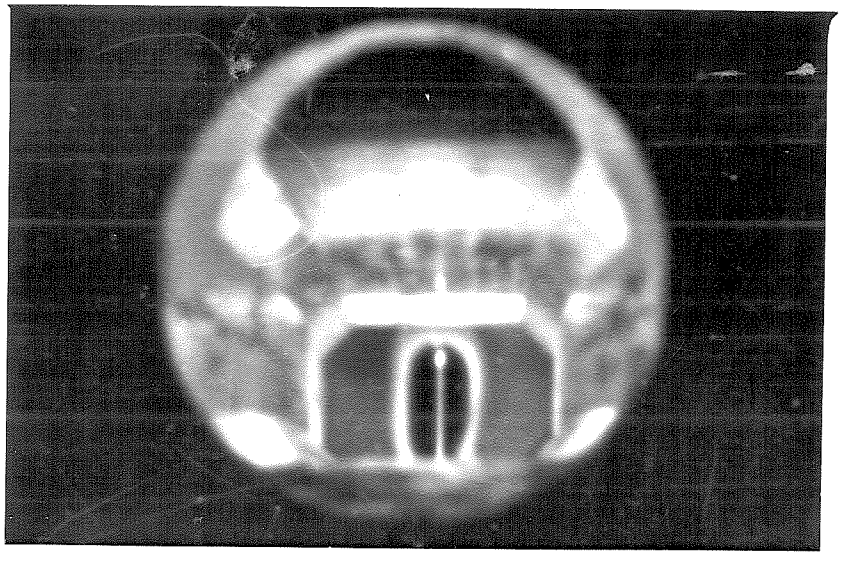

Fig. 26 - Distinct mist first appears outside of halo - side view.

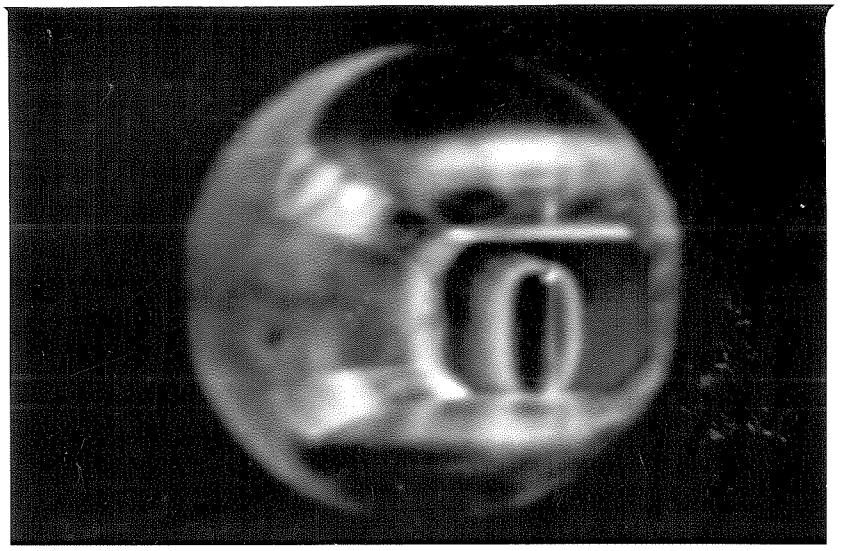

Fig. 27 - Distinct mist first appears outside of halo - end view.

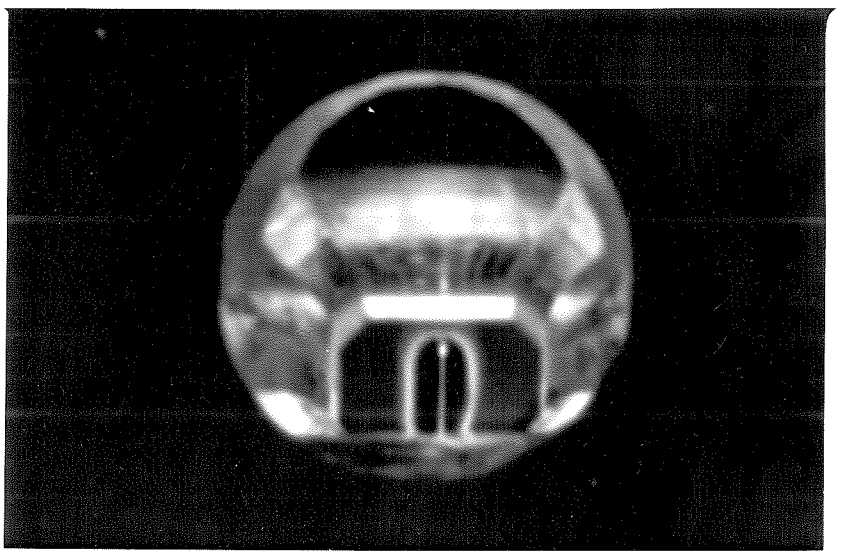

Fig. 28 - Slightly faster than Figs. 26 and 27. Mist outside of halo less distinct.

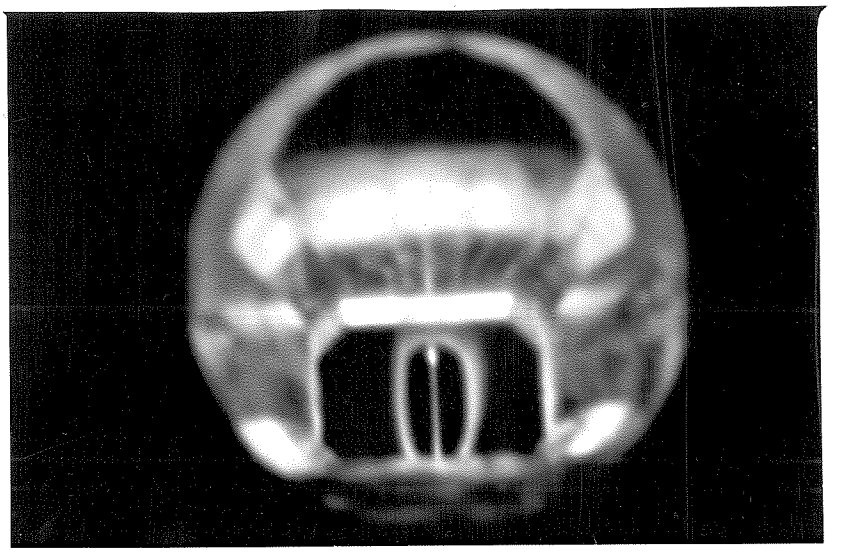

Fig. 29 - Highest speed.

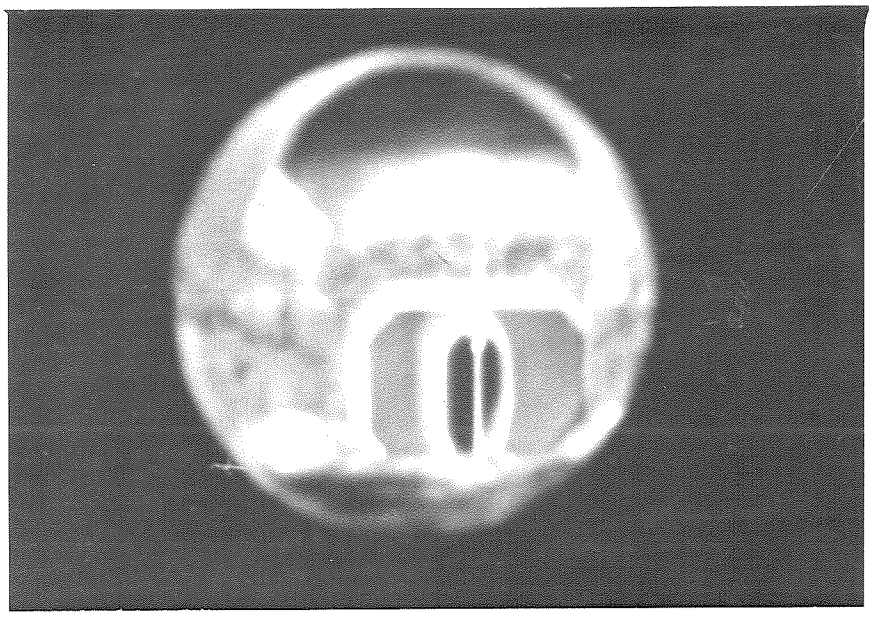

Fig. 30 - Same as Fig. 29 but taken just after starting compressor when there is an unusually high moisture content in the air. After several minutes running this would appear like Fig. 29.

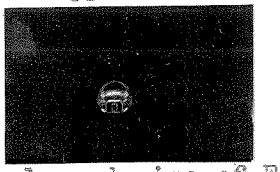

Fig. 31 - Unenlarged size of Figs. 23 - 30.